A human depression circuit derived from focal brain lesions

Jaya L. Padmanabhan, MD[1,2,3]; Danielle Cooke, BS[2], Juho Joutsa, MD PhD [2,4,5]; Shan H. Siddiqi, MD[1,2,3,6,7], Michael Ferguson, PhD[2], R. Ryan Darby, MD[8]; Louis Soussand M.S.[2], Andreas Horn, MD PhD[9]; Na Young Kim, MD PhD[2,10]; Joel L. Voss, PhD[11,12]; Andrew M. Naidech, MD[11,12]; Amy Brodtmann, MBBS PhD[13,14]; Natalia Egorova, PhD[13,14]; Sophia Gozzi, DPsych(Clinical)[15,16]; Thanh G Phan, MBBS PhD[15,16]; Maurizio Corbetta, MD[17,18]; Jordan Grafman, PhD[19,20] , Michael D. Fox, MD PhD[2,3]

[1] Department of Psychiatry, Beth Israel Deaconess Medical Center, Boston, MA
[2] Berenson-Allen Center for Non-Invasive Brain Stimulation, Department of Neurology, Beth Israel Deaconess Medical Center, Harvard Medical School, Boston, MA
[3] Division of Cognitive Neurology, Department of Neurology, Beth Israel Deaconess Medical Center, Harvard Medical School, Boston, MA
[4] Department of Neurology, University of Turku, Turku, Finland
[5] Division of Clinical Neurosciences, Turku University Hospital, Turku, Finland
[6] Division of Neurotherapeutics, McLean Hospital, Harvard Medical School, Belmont, MA
[7] Center for Neuroscience & Regenerative Medicine, Uniformed Services University of the Health Sciences, Bethesda, MD
[8] Department of Neurology, Vanderbilt University Medical Center, Nashville TN
[9] Movement Disorders and Neuromodulation Unit, Department of Neurology, Charité – University Medicine Berlin
[10] Department and Research Institute of Rehabilitation Medicine, Yonsei University College of Medicine, Seoul, Republic of Korea
[11] Ken & Ruth Davee Department of Neurology, Feinberg School of Medicine, Northwestern University, Chicago, IL
[12] Department of Medical Social Sciences, Feinberg School of Medicine, Northwestern University, Chicago, IL
[13]Florey Institute of Neuroscience and Mental Health, Melbourne, Australia
[14] Melbourne School of Psychological Sciences, University of Melbourne, Melbourne, Australia
[15] School of Psychological Sciences, Department of Medicine, Monash University, Melbourne, VIC, Australia
[16] Stroke and Aging Research Group, School of Clinical Sciences, Department of Medicine, Monash University and Stroke Unit, Monash Medical Centre, Melbourne, VIC, Australia
[17] Department of Neuroscience, University of Padova and Padova Neuroscience Center, Padova, Italy
[18] Departments of Neurology, Radiology, Bioengineering, Neuroscience, Washington University School of Medicine, Saint Louis, MO, USA
[19] Psychiatry and Behavioral Sciences & Cognitive Neurology/Alzheimer's Disease Research Center, Feinberg School of Medicine and Department of Psychology, Northwestern University, Chicago, IL
[20] Shirley Ryan AbilityLab, Chicago, IL

Corresponding Authors: Jaya Padmanabhan, MD and Michael D. Fox, MD PhD

Beth Israel Deaconess Medical Center
330 Brookline Avenue
Boston, MA 02215
Email: foxmdphd@gmail.com
Ph: 617-319-9737
Fax: 617-667-7981

Running title: Lesion network mapping of depression
Key Words: depression, lesion, functional connectivity, network, functional MRI, imaging, stroke
Abstract Word Count: 246 words
Main Text Word Count: 3999 words
Number of Figures: 5
Number of Tables: 1

Abstract:

Background: Focal brain lesions can lend insight into the causal neuroanatomical substrate of depression in the human brain. However, studies of lesion location have led to inconsistent results.

Methods: Five independent datasets with different lesion etiologies and measures of post-lesion depression were collated (N = 461). Each 3D lesion location was mapped to a common brain atlas. We used voxel lesion symptom mapping to test for associations between depression and lesion locations. Next, we computed the network of regions functionally connected to each lesion location using a large normative connectome dataset (N = 1000). We used these lesion network maps to test for associations between depression and connected brain circuits. Reproducibility was assessed using a rigorous leave-one-dataset-out validation. Finally, we tested whether lesion locations associated with depression fell within the same circuit as brain stimulation sites effective for improving post-stroke depression.

Results: Lesion locations associated with depression were highly heterogeneous, and no single brain region was consistently implicated. However, these same lesion locations mapped to a connected brain circuit, centered on the left dorsolateral prefrontal cortex. Results were robust to leave one-dataset-out cross-validation. Finally, our depression circuit derived from brain lesions aligned with brain stimulation sites effective for improving post-stroke depression.

Conclusions: Lesion locations associated with depression fail to map to a specific brain region but do map to a specific brain circuit. This circuit may have prognostic utility in identifying patients at risk for post-stroke depression and therapeutic utility in refining brain stimulation targets.

Introduction:

Patients with focal brain lesions can yield insight into the causal neuroanatomical substrate underlying neuropsychiatric symptoms (1, 2). Several decades ago, an association between left frontal lesions and depression was reported for both stroke (3, 4) and brain tumors (5, 6). Subsequent work refined this association to lesions in the bilateral dorsolateral prefrontal cortex (DLPFC) (7). These lesion localization studies are important as depression is an independent predictor of morbidity and mortality post-stroke (8). These lesion studies are also important for the insight they provide into the neuroanatomy underlying primary depression, including identification of treatment targets. For example, the first trials of transcranial magnetic stimulation (TMS) to the left DLPFC for treatment of primary depression were motivated partly by lesion data (9, 10).

However, localization of depression based on focal brain lesions has been inconsistent. Even the early studies noted that most patients with post-stroke depression had lesions outside the left frontal cortex (3, 4). Work aimed at replicating this association found it only held true for specific time points (11), or not at all (12). Multiple meta-analyses have failed to find an association between left frontal lesions and depression (13-16). Studies using newer methods such as voxel-based lesion-symptom mapping have also failed to find lesion locations significantly associated with depression (17, 18).

One potential reason for these inconsistent findings is that lesions causing similar symptoms may localize to connected brain networks rather than individual brain regions (19). Similarly, symptoms caused by focal brain lesions can arise from brain regions connected to the lesion location rather than the lesion location itself, a phenomenon termed diaschisis (20, 21). A recently validated technique called lesion network mapping can better account for these factors and incorporate them into lesion-based localization (19, 22-25). This method uses lesion locations as seed regions in resting state functional connectivity analyses, taking advantage of connectome data from large cohorts of healthy subjects. By comparing the functional

connectivity profiles of lesions associated with a particular symptom, this method can identify brain regions or networks underlying a symptom of interest. This technique has proven useful for understanding hallucinations (19), delusions (22), criminality (26), and even disorders of free will (27).

In this study, we analyzed the association of lesion location with depression across 5 independent lesion data sets and several lesion etiologies (ischemic stroke, intracerebral hemorrhage, and penetrating traumatic brain injury) (7, 17, 28-30). We hypothesized that lesion location alone would not be significantly associated with depression but that resting-state functional connectivity between the lesion location and other brain regions would be.

Methods and Materials:

Subjects and Lesions:

This study was approved by the institutional review board at Beth Israel Deaconess Medical Center (protocol number: 2018P000128). We performed a systematic literature search to identify lesion data sets containing depression assessments and wrote to investigators to request data (Supplementary Methods). Five independent lesion data sets totaling 461 patients were included with varied lesion etiologies, depression scales, and timing of depression assessment (Table 1, Figure 1, Supplementary Methods) (7, 17, 28-30). Our primary analysis focused on patients with moderate to severe depression (N = 58) versus patients with no depression (N = 300, referred to subsequently as 'controls' or 'non-depressed controls') using established cutoffs for each depression scale (Supplementary Methods, Table 1) (7, 17, 31-36). We used a binary contrast of "depressed" versus "non-depressed" for our main analysis for three reasons. First, this maintains consistency with the post-stroke depression literature, including studies whose findings we sought to replicate (7, 37, 38). Second, this enables combining datasets with different depression measures, each of which has established cutoffs for binary classification. Finally, because depression scales can be influenced by many factors,

focusing on the extremes may be more likely to identify associations with lesion location. However, we also repeated our analyses on the full cohort of lesions (N = 461) treating depression as a continuous measure. In order to perform analyses across datasets, depression scores for subjects within each dataset were z-scored against other subjects within that same dataset, yielding a normalized continuous depression score for each subject.

Lesions were manually segmented based on CT (7, 29) or structural MRI images (17, 28, 30), spatially normalized to MNI152 atlas space, and binarized, such that voxels within the lesion carried a value of 1, and all other voxels carried a value of 0. Lesion masks were added together to create lesion overlap maps (Supplementary Figure S1).

Analysis of Lesion Location:

To identify any lesioned brain voxels associated with depression, we performed voxel-based lesion symptom mapping (VLSM) (1, 2) using the Matlab package NiiStat (https://github.com/neurolabusc/NiiStat), controlling for lesion size and dataset as covariates (39) and using standard settings and statistical cutoffs (Supplementary Methods) (1, 2). To maximize sensitivity, we focused our analysis on the bilateral dorsal lateral prefrontal cortex (DLPFC), defined using the Harvard Oxford atlas “middle frontal gyrus” (MFG) region and a cutoff of >0% probability. This focus was motivated by literature implicating the DLPFC in depression and its use as a treatment target for TMS. To ensure results were not dependent on our choice of ROI, we repeated our analysis using two other DLPFC ROIs used in prior studies of lesion location and depression (4, 7) (Supplementary Figure S2). To ensure that we did not miss important results outside the DLPFC, we repeated our analysis using no mask (i.e., including the whole brain). Finally, we repeated analyses treating depression as a continuous rather than a binary variable and including all lesions (N = 461).

In addition to the above voxel-wise analyses, we also replicated ROI-based analyses from prior studies that reported positive associations between lesion location and depression (4,

7) and tested for associations between depression and lesions to the left versus right hemisphere (Supplementary Methods, Supplementary Figure S2). In total, we tested seven *a priori* hypotheses regarding lesion intersection with these ROIs.

Lesion Network Mapping:

Using previously validated methods for lesion network mapping (19, 22), we tested whether lesions associated with depression mapped to a connected brain circuit. Functional connectivity between each lesion location and all other brain voxels was computed using resting state functional connectivity data from 1000 healthy subjects (40, 41) (Figure 2, Supplementary Methods).

Unthresholded lesion network maps of depressed (N = 58) versus non-depressed control (N = 300) subjects were statistically compared using a general linear model and permutation testing (Permutation Analysis of Linear Models in FSL 3.2.0), including dataset and lesion size as covariates (42, 43). The location of each lesion was not excluded from the corresponding lesion network map. As in our VLSM analysis, we searched for significant results within the Harvard Oxford bilateral MFG mask. We used a conservative voxel-level family-wise error correction for multiple comparisons, correcting for all brain voxels within our mask ($p_c <$ 0.05). This is more stringent than the commonly used cluster-based correction which can be associated with false positives depending on the detection threshold (44). As with our VLSM analysis, we repeated our analysis using two other DLPFC masks and using no mask at all (Supplementary Methods).

Significant voxels from this analysis were extracted as a seed region of interest, and the functional connectivity of this region to the rest of the brain was computed using the normative connectome of 1000 healthy subjects. By definition this network map, which we term the "depression circuit", best encompasses lesion locations associated with depression while avoiding lesion locations that are not.

We repeated this analysis using the subset of lesions with a common lesion etiology (ischemic stroke, hemorrhagic stroke, penetrating traumatic brain injury) and the subset of lesions with a confirmed lack of history of depression pre-lesion. Similarity to our primary circuit (N = 358) was assessed through spatial correlation (Supplementary Methods).

Leave-one-dataset-out cross-validation and network damage scores:

To ensure that our findings were not biased by any one of our five datasets, and to test whether our depression circuit could predict depression in independent datasets, we performed a leave-one-dataset-out validation. We statistically compared the lesion network maps of depressed and control subjects five times, each time leaving out one of the five datasets. Each time, voxels that survived voxel-wise FWE correction were extracted as regions of interest (Figure 3A).

Then, we used each of these five regions of interest as seeds and computed their functional connectivity with the rest of the brain using our normative connectome dataset (N = 1000). This generated five different 'depression circuit' maps (Figure 3B and 3C). We then assigned each subject a 'network damage score' using the depression circuit that was generated from the other four datasets to which the lesion did not belong (Figure 3). Each subject's 'network damage score' was calculated by summing the intensity (T values) of those voxels in the depression circuit that overlapped with that subject's lesion. To avoid bias associated with a choice of threshold, network damage scores were computed using unthresholded depression circuit maps. To control for lesion size and dataset, we regressed this score against these variables and extracted the residuals to create an adjusted network damage score, which was used in all analyses.

First, we examined whether the network damage score differed between depressed and control subjects. Second, we examined whether subjects with higher network damage scores were more likely to have depression. Due to the network damage score's non-normality,

statistical significance for these analyses were calculated using permutation testing with one million permutations, a non-parametric procedure that can be used on non-normal data (45) (Supplementary Methods).

To ensure that results were not overly dependent on the cutoff values used to define control and depressed subjects, we performed additional analyses on the full cohort of subjects (N = 461) using the continuous depression score. We performed a Pearson's correlation between this score and the network damage score, using permutation testing to determine statistical significance due to non-normality of both variables. We also examined whether lesion size predicted depression in binary and continuous models of depression.

We then divided subjects into three risk categories: low risk (network damage score < 2 SD below the mean), high risk (network damage score > 2 SD above the mean), and medium risk (the remaining subjects). Mean depression scores were compared across risk categories using one-way analysis of variance (Figure 4A). Finally, we grouped subjects with mild or questionable depression along with control subjects, and evaluated whether the prevalence of depression differed among the three risk categories using a chi-squared test (Figure 4B).

Post-stroke Depression Treatment Targets:

From the literature, we identified TMS targets that have successfully been used to treat depression following strokes (Supplementary Methods). We constructed 12 mm cone models of TMS activation for each TMS target and masked them against the MNI brain, as described in prior work (46). As a control, we also constructed a 12 mm cone model centered around the vertex (equivalent to Cz electrode location in the 10/20 EEG system), commonly used as a control target in trials of TMS and shown not to improve depression. Using normative connectome data, we assessed whether the successful TMS targets showed positive functional connectivity with the seed identified in our lesion network mapping analysis ('LNM results' in Figure 2B). We then assessed whether the successful TMS targets showed significantly greater

functional connectivity to the results of our lesion network mapping analysis than the vertex using Hotelling's t-test (Figure 5; (47)).

Results:

Analysis of Lesion Location

Across our five datasets (Table 1), lesions associated with moderate to severe depression and lesions associated with no depression occurred in various brain locations (Figure 1). Only 8 of 58 lesions associated with depression overlapped in any one location (Supplementary Figure S1A). Using voxel-based lesion-symptom mapping on the pooled data, no lesioned voxels were significantly associated with depression, either inside our DLPFC ROIs or in a whole brain analysis (1) (Supplementary Table S1, Figure 2A) . There were also no significant voxel-based associations when treating depression as a continuous variable (N = 461), either inside or outside our DLPFC ROIs.

Finally, we found no significant association between lesion location and depression when repeating ROI-based analyses from prior papers (4, 7) or when performing laterality analyses (Supplementary Materials). Specifically, there was no difference in depression prevalence comparing left anterior versus left posterior lesions ($p = 0.36$), left anterior versus right anterior lesions ($p = 0.32$), right anterior versus right posterior lesions ($p = 1$), bilateral dorsal lateral prefrontal versus bilateral ventral medial prefrontal lesions ($p = 1$), or bilateral dorsal lateral prefrontal and non-prefrontal lesions ($p = 0.76$). There was also no difference in depression prevalence between left- and right-sided lesions in the cerebral hemispheres ($p = 1$), or between lesions falling within the Harvard Oxford left MFG and right MFG ($p = 0.44$) (Supplementary Table S2).

Lesion Network Mapping

Functional connectivity between each lesion location and the whole brain was computed using a normative connectome (Figure 2B). In contrast to analyses focused on lesion location alone, lesion connectivity was significantly associated with depression. Specifically, a focal region in the left DLPFC was significantly more connected to lesions of depressed subjects compared to non-depressed subjects (159 voxels surviving voxel-level family-wise error [FWE] correction $p_c < 0.05$). The peak of this left DLPFC region was highly significant ($p_c = 0.005$) and located at the grey-white matter junction (MNI coordinates: x = -32, y = 12, z = 36, Figure 2B). This result was independent of the specific DLPFC mask (Supplementary Figure S2) and the peak remained significant in a whole brain analysis ($p_c < 0.05$). No other significant peaks outside the left DLPFC were identified.

By definition, functional connectivity with this DLPFC region defines a human brain circuit that encompasses lesion locations associated with depression while avoiding lesion locations that are not (Figure 2C; Supplementary Table S3). Lesion locations from patients with depression will intersect positively connected brain regions in this circuit, while lesions from non-depressed subjects will intersect neutral or negatively connected regions in this circuit. This lesion-based depression circuit was similar when restricted to cases of hemorrhagic stroke (r = 0.66), ischemic stroke (r = 0.52), penetrating traumatic brain injury (r = 0.95), or a documented lack of depression prior to the lesion (r = 0.53) (Supplementary Figures S3 and S4).

Leave-one-dataset-out cross-validation and network damage scores:

As a rigorous test of reproducibility, we repeated the above analysis 5 times, each time excluding one dataset. Lesions associated with depression were always more connected to a focal region in the left DLPFC ($p_c < 0.05$) that was similar no matter which dataset was excluded (Figure 3A). Connectivity with this left DLPFC region of interest defined a brain circuit that was similar no matter which dataset was excluded (average spatial correlation r = 0.91, Figure 3B, Supplementary Table S4). Lesions associated with depression intersected this circuit to a

significantly greater degree than control lesions ($p = 0.0013$), as demonstrated by a higher network damage score. The degree to which lesions intersected this circuit predicted depression status (OR = 1.62, $p = 0.0035$). Lesion size alone did not predict depression status (OR = 1.14, $p = 0.31$).

To ensure these results were not dependent on the cutoffs used to classify patients as "depressed" or "not depressed", we repeated this analysis of circuit intersection on our full cohort of patients (n = 461) treating depression as a continuous rather than a binary variable. Intersection with our depression circuit (defined using the other four datasets) was a significant predictor of continuous depression severity ($r = 0.13$, $p = 0.0040$). Lesion size alone did not predict continuous depression severity ($r = 0.061$, $p = 0.19$).

Binning all 461 subjects into three risk categories based on circuit intersection revealed a significant difference in continuous depression scores ($F(2,458) = 4.8$, $p = 0.0036$, Figure 4A) and depression prevalence ($X^2 = 7.2$, $p = 0.019$, Figure 4B). Prevalence of depression was four times higher (35.7%) in the high-risk category compared to the low-risk category (8.3%).

Post-stroke Depression Treatment Targets:

We identified three TMS targets with evidence of efficacy in treating post-stroke depression (Figure 5). These included the 5 cm target traditionally also used in treatment of primary depression (48, 49), the left F3 electrode location on the scalp using the 10/20 EEG coordinate system (50, 51), and the center of the left MFG (52). All three targets fell within our depression circuit derived from focal brain lesions, defined by positive connectivity to our node in the left DLPFC ($r = 0.23$ for the 5 cm target, $r = 0.14$ for the EEG F3 target, and $r = 0.20$ for the center of the MFG, all $p < 0.00001$). All three TMS targets were significantly more connected to this DLPFC node than our control site in the vertex ($p < 0.0001$ for all comparisons).

Discussion:

Our results define a depression circuit in the human brain based on brain lesions. First, we found that lesion location alone was not significantly associated with depression. Second, we showed that functional connectivity between lesion locations and the left DLPFC was strongly associated with depression, independent of lesion etiology, lesion size or dataset. Third, we validated our depression circuit by predicting depression status and depression severity in independent lesion cohorts. Finally, we showed that our circuit derived from brain lesions associated with depression aligns with brain stimulation sites that improve depression, suggesting therapeutic utility. Although we used binary cutoffs for our main analysis, our findings are not dependent on these cutoffs and were reproducible when treating depression as a continuous measure.

Lesion Location and Depression:

We did not find an association between lesion location and depression anywhere in the brain using either VLSM or when replicating prior positive analyses from the literature (4, 7). While it is possible that significant associations would have become apparent with more lesions and statistical power, this study is the largest VLSM analysis of depression to date, about twice the size of the next largest study (18). Other studies approaching the size of our study, but classifying lesion location based on rough anatomical descriptions rather than lesioned voxels, have also been negative (53), including multiple meta-analyses (12-15). Collectively, these results suggest that lesions associated with depression do not localize to any specific brain region.

Lesion Network Mapping, Frontal Connectivity and Depression:

In contrast to the negative results regarding lesion location, functional connectivity between lesion locations and the rest of the brain was a significant predictor of depression. This

finding is consistent with a growing literature suggesting that symptoms localize to connected brain circuits, not single brain lesions (19, 22, 54-56).

Functional connectivity between lesion location and a region within the left DLPFC was higher in depressed than in non-depressed subjects, a finding that remained significant even in a conservative whole-brain analysis with voxel-wise FWE correction. Because this analysis compared lesions from depressed individuals with non-depressed individuals, we control for the possibility that the DLPFC is simply a hub connected to all lesion locations. These findings are consistent with lesion studies implicating the DLPFC in depression (4, 7). However, our findings also help explain why multiple lesion studies, including the present study, failed to see such relationships (12-15). Specifically, our results suggest that lesions located outside the DLPFC, but functionally connected to this area, can also cause depression.

Connectivity with the DLPFC defines a human brain circuit that best encompasses lesion locations associated with depression. This circuit was independent of lesion etiology, dataset, or scale used to measure depression. Intersection between lesion location and this circuit predicted prevalence and severity of depression in independent lesion cohorts. As such, this circuit might be used to identify patients who are at elevated risk of depression after a stroke or brain injury. Clinicians could examine the overlap between a patient's lesion and our depression circuit, and patients at elevated risk could then be directed towards early psychiatric evaluation and treatment.

Our circuit derived from brain lesions associated with depression aligned with stimulation sites found to improve depression in post-stroke depression. Although previous work has suggested therapeutic relevance of lesion network mapping results (57-59), this is the first study to show that lesions causing a symptom are part of the same brain circuit as stimulation sites improving that symptom in lesion patients. While the peak of our lesion-based depression circuit is in the left DLPFC, TMS to secondary nodes in this circuit may also be beneficial, although this

remains a testable hypothesis for future work. These results support the use of lesion network mapping to identify therapeutic brain stimulation targets for improving lesion-induced symptoms.

It is likely that our depression circuit has implications for understanding and treating primary depression not caused by focal brain lesions. While depression has not consistently been associated with changes in DLPFC activity (60, 61), increases in DLPFC activity have been associated with antidepressant response (62), especially improvement in the cognitive symptoms of depression (63). However, it is now widely recognized that primary depression is associated with circuit abnormalities that extend beyond the DLPFC (64, 65). Our circuit, based on causal brain lesions, may help refine circuit models of primary depression.

Finally, our results may help inform treatment targets in primary depression. The DLPFC region was initially chosen as a TMS target for primary depression based partly on lesion studies (66). Our current depression circuit may help refine this target and motivate new strategies for neuromodulation that target a brain circuit rather than a single brain region (67, 68).

Limitations and Future Directions:

There are several limitations. First, as previously discussed (22), lesion network mapping using a normative data set assumes that the patterns of connectivity in healthy individuals are approximately the same as for an individual patient prior to their brain lesion. This assumption appears reasonable given the success of lesion network mapping across numerous symptoms (19, 22-25) and the fact that prior work using a connectome age-matched to lesion patients had no effect on results (19). In similar work on TMS- or DBS-electrodes, disease-matching the connectomes also had no effect on results (25, 69). Second, the current study focused only on lesion location and connectivity to explain lesion-associated depression. We did not account for compensatory network adaptations that may occur following a lesion nor

did we account for many other factors that contribute to post-lesion depression such as genetics, psychosocial situation, degree of disability, or co-morbid diagnosis (14). Third, lesions were treated as functionally homogenous units regardless of their size. A potential approach to address this limitation could involve deconstructing lesions into functionally homogenous seeds using an atlas, and then using these seeds to generate multiple lesion network maps for each subject. However, as this potential approach has not been standardized, we elected to pursue our previously validated approach.

Fourth, we did not have complete information about psychiatric comorbidities or pre-lesion history of depression. Substance dependence and post-traumatic stress disorder can be significant co-morbidities in veterans with penetrating traumatic brain injury, for example. Additionally, the time point of depression assessment relative to the lesion was variable across datasets, limiting our ability to make strong causal inferences. At least some patients in this study likely had depression that was unrelated to the location of their brain damage. However, a depression circuit created from the subset of individuals who had a documented lack of depression prior to their lesion was similar to our primary depression circuit ($r = 0.53$). Fifth, depression is a syndrome composed of many different symptoms with potentially distinct neuroanatomical correlates. Future work applying this technique to individual symptoms of depression is needed. Sixth, our results should not be interpreted as specific to the left DLPFC relative to the right DLPFC. Although connectivity to the left DLPFC was the only significant finding in our full cohort, some sub-cohorts showed similar findings in the right DLPFC (Supplementary Figures S3 and S4). Finally, there is certain to be some error in lesion tracing and atlas registrations. However, it is important to note that all of these limitations should bias us against the present findings, namely consistent localization of lesions associated with depression to a specific brain circuit across datasets and lesion etiologies.

Acknowledgements:

Funding/Support: This work was supported in part by funding from the Sidney R. Baer, Jr. Foundation (to J.L.P., R.R.D., S.H.S., and M.D.F.), the Harvard Medical School Department of Psychiatry Dupont-Warren Award (to J.L.P.), the American Psychiatric Association Kempf Award (to J.L.P.), the Alzheimer's Association Clinical Fellowship Program (to R.R.D.), the BrightFocus Foundation Alzheimer's Disease Research Program (to R.R.D.), the Vanderbilt Faculty Research Scholars Award (to R.R.D.), the Academy of Finland grant #295580 (to J.J.), and the National Institutes of Health Grants R01MH113929 and K23NS083741 (to M.D.F.). All funding agencies had no role in the study design, collection, management, analysis, interpretation, preparation, review, interpretation, or submission of this article.

Disclosures: The authors report no biomedical financial interests or potential conflicts of interest.

Supplementary information is available at *Biological Psychiatry*'s website.

References:

1. Karnath HO, Sperber C, Rorden C (2018): Mapping human brain lesions and their functional consequences. *Neuroimage*. 165:180-189.
2. Rorden C, Karnath HO, Bonilha L (2007): Improving lesion-symptom mapping. *J Cogn Neurosci*. 19:1081-1088.
3. Robinson RG, Price TR (1982): Post-stroke depressive disorders: a follow-up study of 103 patients. *Stroke; a journal of cerebral circulation*. 13:635-641.
4. Robinson RG, Kubos KL, Starr LB, Rao K, Price TR (1984): Mood disorders in stroke patients. Importance of location of lesion. *Brain*. 107 (Pt 1):81-93.
5. Wellisch DK, Kaleita TA, Freeman D, Cloughesy T, Goldman J (2002): Predicting major depression in brain tumor patients. *Psychooncology*. 11:230-238.
6. Belyi BI (1987): Mental impairment in unilateral frontal tumours: role of the laterality of the lesion. *Int J Neurosci*. 32:799-810.
7. Koenigs M, Huey ED, Calamia M, Raymont V, Tranel D, Grafman J (2008): Distinct regions of prefrontal cortex mediate resistance and vulnerability to depression. *J Neurosci*. 28:12341-12348.
8. Everson SA, Roberts RE, Goldberg DE, Kaplan GA (1998): Depressive symptoms and increased risk of stroke mortality over a 29-year period. *Arch Intern Med*. 158:1133-1138.
9. George MS, Nahas Z, Molloy M, Speer AM, Oliver NC, Li XB, et al. (2000): A controlled trial of daily left prefrontal cortex TMS for treating depression. *Biol Psychiatry*. 48:962-970.
10. Pascual-Leone A, Rubio B, Pallardo F, Catala MD (1996): Rapid-rate transcranial magnetic stimulation of left dorsolateral prefrontal cortex in drug-resistant depression. *Lancet*. 348:233-237.
11. Narushima K, Kosier JT, Robinson RG (2003): A reappraisal of poststroke depression, intra- and inter-hemispheric lesion location using meta-analysis. *J Neuropsychiatry Clin Neurosci*. 15:422-430.
12. Kutlubaev MA, Hackett ML (2014): Part II: predictors of depression after stroke and impact of depression on stroke outcome: an updated systematic review of observational studies. *Int J Stroke*. 9:1026-1036.
13. Wei N, Yong W, Li X, Zhou Y, Deng M, Zhu H, et al. (2015): Post-stroke depression and lesion location: a systematic review. *Journal of neurology*. 262:81-90.
14. Ayerbe L, Ayis S, Wolfe CD, Rudd AG (2013): Natural history, predictors and outcomes of depression after stroke: systematic review and meta-analysis. *Br J Psychiatry*. 202:14-21.
15. Yu L, Liu CK, Chen JW, Wang SY, Wu YH, Yu SH (2004): Relationship between post-stroke depression and lesion location: a meta-analysis. *Kaohsiung J Med Sci*. 20:372-380.
16. Rooney AG, Carson A, Grant R (2011): Depression in cerebral glioma patients: a systematic review of observational studies. *J Natl Cancer Inst*. 103:61-76.
17. Gozzi SA, Wood AG, Chen J, Vaddadi K, Phan TG (2014): Imaging predictors of poststroke depression: methodological factors in voxel-based analysis. *BMJ Open*. 4:e004948.
18. Sagnier S, Munsch F, Bigourdan A, Debruxelles S, Poli M, Renou P, et al. (2019): The Influence of Stroke Location on Cognitive and Mood Impairment. A Voxel-Based Lesion-Symptom Mapping Study. *J Stroke Cerebrovasc Dis*. 28:1236-1242.

19. Boes AD, Prasad S, Liu H, Liu Q, Pascual-Leone A, Caviness VS, Jr., et al. (2015): Network localization of neurological symptoms from focal brain lesions. *Brain*. 138:3061-3075.
20. van Meer MP, van der Marel K, Wang K, Otte WM, El Bouazati S, Roeling TA, et al. (2010): Recovery of sensorimotor function after experimental stroke correlates with restoration of resting-state interhemispheric functional connectivity. *J Neurosci*. 30:3964-3972.
21. Carrera E, Tononi G (2014): Diaschisis: past, present, future. *Brain*. 137:2408-2422.
22. Darby RR, Laganiere S, Pascual-Leone A, Prasad S, Fox MD (2017): Finding the imposter: brain connectivity of lesions causing delusional misidentifications. *Brain*. 140:497-507.
23. Laganiere S, Boes AD, Fox MD (2016): Network localization of hemichorea-hemiballismus. *Neurology*. 86:2187-2195.
24. Fischer DB, Boes AD, Demertzi A, Evrard HC, Laureys S, Edlow BL, et al. (2016): A human brain network derived from coma-causing brainstem lesions. *Neurology*. 87:2427-2434.
25. Horn A, Reich M, Vorwerk J, Li N, Wenzel G, Fang Q, et al. (2017): Connectivity Predicts deep brain stimulation outcome in Parkinson disease. *Ann Neurol*. 82:67-78.
26. Darby RR, Horn A, Cushman F, Fox MD (2018): Lesion network localization of criminal behavior. *Proc Natl Acad Sci U S A*. 115:601-606.
27. Darby RR, Joutsa J, Burke MJ, Fox MD (2018): Lesion network localization of free will. *Proc Natl Acad Sci U S A*. 115:10792-10797.
28. Corbetta M, Ramsey L, Callejas A, Baldassarre A, Hacker CD, Siegel JS, et al. (2015): Common behavioral clusters and subcortical anatomy in stroke. *Neuron*. 85:927-941.
29. Naidech AM, Polnaszek KL, Berman MD, Voss JL (2016): Hematoma Locations Predicting Delirium Symptoms After Intracerebral Hemorrhage. *Neurocrit Care*. 24:397-403.
30. Egorova N, Cumming T, Shirbin C, Veldsman M, Werden E, Brodtmann A (2018): Lower cognitive control network connectivity in stroke participants with depressive features. *Transl Psychiatry*. 7:4.
31. Gershon RC, Lai JS, Bode R, Choi S, Moy C, Bleck T, et al. (2012): Neuro-QOL: quality of life item banks for adults with neurological disorders: item development and calibrations based upon clinical and general population testing. *Quality of life research : an international journal of quality of life aspects of treatment, care and rehabilitation*. 21:475-486.
32. Burke WJ, Roccaforte WH, Wengel SP (1991): The short form of the Geriatric Depression Scale: a comparison with the 30-item form. *J Geriatr Psychiatry Neurol*. 4:173-178.
33. Kroenke K, Spitzer RL, Williams JB (2001): The PHQ-9: validity of a brief depression severity measure. *J Gen Intern Med*. 16:606-613.
34. Zigmond AS, Snaith RP (1983): The hospital anxiety and depression scale. *Acta Psychiatr Scand*. 67:361-370.
35. Sheehan DV, Lecrubier Y, Sheehan KH, Amorim P, Janavs J, Weiller E, et al. (1998): The Mini-International Neuropsychiatric Interview (M.I.N.I.): the development and validation of a structured diagnostic psychiatric interview for DSM-IV and ICD-10. *J Clin Psychiatry*. 59 Suppl 20:22-33;quiz 34-57.
36. Beck AT, Steer RA, Brown G (1996): Manual for the Beck Depression Inventory-II. San Antonion, TX: Psychological Corporation.
37. Zhang Y, Zhao H, Fang Y, Wang S, Zhou H (2017): The association between lesion location, sex and poststroke depression: Meta-analysis. *Brain Behav*. 7:e00788.

38. Carson AJ, MacHale S, Allen K, Lawrie SM, Dennis M, House A, et al. (2000): Depression after stroke and lesion location: a systematic review. *Lancet*. 356:122-126.
39. Stark BC, Yourganov G, Rorden C (2018): User Manual and Tutorial for NiiStat. http://wwwnitrcorg/projects/niistat.
40. Holmes AJ, Hollinshead MO, O'Keefe TM, Petrov VI, Fariello GR, Wald LL, et al. (2015): Brain Genomics Superstruct Project initial data release with structural, functional, and behavioral measures. *Sci Data*. 2:150031.
41. Yeo BT, Krienen FM, Sepulcre J, Sabuncu MR, Lashkari D, Hollinshead M, et al. (2011): The organization of the human cerebral cortex estimated by intrinsic functional connectivity. *J Neurophysiol*. 106:1125-1165.
42. Winkler AM, Ridgway GR, Webster MA, Smith SM, Nichols TE (2014): Permutation inference for the general linear model. *Neuroimage*. 92:381-397.
43. The MathWorks I (2015): MATLAB and Statistics Toolbox Release 2015b. Natick, Massachusetts.
44. Eklund A, Nichols TE, Knutsson H (2016): Cluster failure: Why fMRI inferences for spatial extent have inflated false-positive rates. *Proc Natl Acad Sci U S A*. 113:7900-7905.
45. Curran-Everett D (2017): Explorations in statistics: the assumption of normality. *Adv Physiol Educ*. 41:449-453.
46. Fox MD, Liu H, Pascual-Leone A (2013): Identification of reproducible individualized targets for treatment of depression with TMS based on intrinsic connectivity. *Neuroimage*. 66:151-160.
47. Diedenhofen B, Musch J (2015): cocor: a comprehensive solution for the statistical comparison of correlations. *PLoS One*. 10:e0121945.
48. VanDerwerker CJ, Ross RE, Stimpson KH, Embry AE, Aaron SE, Cence B, et al. (2018): Combining therapeutic approaches: rTMS and aerobic exercise in post-stroke depression: a case series. *Top Stroke Rehabil*. 25:61-67.
49. El Etribi A, El Nahas N, Nagy N, Nabil H (2010): Repetitive transcranial magnetic stimulation in post stroke depression. *Current Psychiatry*. 17:9-14.
50. Gu SY, Chang MC (2017): The Effects of 10-Hz Repetitive Transcranial Magnetic Stimulation on Depression in Chronic Stroke Patients. *Brain stimulation*. 10:270-274.
51. Kim BR, Kim DY, Chun MH, Yi JH, Kwon JS (2010): Effect of repetitive transcranial magnetic stimulation on cognition and mood in stroke patients: a double-blind, sham-controlled trial. *Am J Phys Med Rehabil*. 89:362-368.
52. Jorge RE, Robinson RG, Tateno A, Narushima K, Acion L, Moser D, et al. (2004): Repetitive transcranial magnetic stimulation as treatment of poststroke depression: a preliminary study. *Biol Psychiatry*. 55:398-405.
53. Snaphaan L, van der Werf S, Kanselaar K, de Leeuw FE (2009): Post-stroke depressive symptoms are associated with post-stroke characteristics. *Cerebrovasc Dis*. 28:551-557.
54. Carter AR, Astafiev SV, Lang CE, Connor LT, Rengachary J, Strube MJ, et al. (2010): Resting interhemispheric functional magnetic resonance imaging connectivity predicts performance after stroke. *Ann Neurol*. 67:365-375.
55. He BJ, Snyder AZ, Vincent JL, Epstein A, Shulman GL, Corbetta M (2007): Breakdown of functional connectivity in frontoparietal networks underlies behavioral deficits in spatial neglect. *Neuron*. 53:905-918.

56. Siegel JS, Ramsey LE, Snyder AZ, Metcalf NV, Chacko RV, Weinberger K, et al. (2016): Disruptions of network connectivity predict impairment in multiple behavioral domains after stroke. *Proc Natl Acad Sci U S A*. 113:E4367-4376.
57. Fox MD (2018): Mapping Symptoms to Brain Networks with the Human Connectome. *N Engl J Med*. 379:2237-2245.
58. Joutsa J, Horn A, Hsu J, Fox MD (2018): Localizing parkinsonism based on focal brain lesions. *Brain*.
59. Joutsa J, Shih LC, Horn A, Reich MM, Wu O, Rost NS, et al. (2018): Identifying therapeutic targets from spontaneous beneficial brain lesions. *Ann Neurol*. 84:153-157.
60. Kaiser RH, Andrews-Hanna JR, Wager TD, Pizzagalli DA (2015): Large-Scale Network Dysfunction in Major Depressive Disorder: A Meta-analysis of Resting-State Functional Connectivity. *JAMA Psychiatry*. 72:603-611.
61. Zhong X, Pu W, Yao S (2016): Functional alterations of fronto-limbic circuit and default mode network systems in first-episode, drug-naive patients with major depressive disorder: A meta-analysis of resting-state fMRI data. *J Affect Disord*. 206:280-286.
62. Fitzgerald PB, Oxley TJ, Laird AR, Kulkarni J, Egan GF, Daskalakis ZJ (2006): An analysis of functional neuroimaging studies of dorsolateral prefrontal cortical activity in depression. *Psychiatry Res*. 148:33-45.
63. Brody AL, Saxena S, Mandelkern MA, Fairbanks LA, Ho ML, Baxter LR (2001): Brain metabolic changes associated with symptom factor improvement in major depressive disorder. *Biol Psychiatry*. 50:171-178.
64. Mayberg HS, Liotti M, Brannan SK, McGinnis S, Mahurin RK, Jerabek PA, et al. (1999): Reciprocal limbic-cortical function and negative mood: converging PET findings in depression and normal sadness. *Am J Psychiatry*. 156:675-682.
65. Mayberg HS, Lozano AM, Voon V, McNeely HE, Seminowicz D, Hamani C, et al. (2005): Deep brain stimulation for treatment-resistant depression. *Neuron*. 45:651-660.
66. Pascual-Leone A, Wassermann EM, Grafman J, Hallett M (1996): The role of the dorsolateral prefrontal cortex in implicit procedural learning. *Exp Brain Res*. 107:479-485.
67. Fischer DB, Fried PJ, Ruffini G, Ripolles O, Salvador R, Banus J, et al. (2017): Multifocal tDCS targeting the resting state motor network increases cortical excitability beyond traditional tDCS targeting unilateral motor cortex. *Neuroimage*. 157:34-44.
68. Ruffini G, Fox MD, Ripolles O, Miranda PC, Pascual-Leone A (2014): Optimization of multifocal transcranial current stimulation for weighted cortical pattern targeting from realistic modeling of electric fields. *Neuroimage*. 89:216-225.
69. Weigand A, Horn A, Caballero R, Cooke D, Stern AP, Taylor SF, et al. (2018): Prospective Validation That Subgenual Connectivity Predicts Antidepressant Efficacy of Transcranial Magnetic Stimulation Sites. *Biol Psychiatry*. 84:28-37.

Figure Captions:

Figure 1: Lesions from depressed and non-depressed subjects from each of our five datasets demonstrate heterogeneity in lesion location: Dataset 1: Naidech et al, 2016 (intracerebral hemorrhage); Dataset 2: Corbetta et al, 2015 (stroke); Dataset 3: Egorova et al, 2018 (stroke); Dataset 4: Gozzi et al, 2004 (stroke); Dataset 5: Koenigs et al, 2008 (penetrating traumatic brain injury).

Figure 2: Lesion locations associated with depression intersect a connected brain circuit, not an individual brain region. (A) A sample lesion from a depressed subject and a non-depressed subject are depicted in green. Standard voxel-based lesion-symptom mapping identified no lesioned voxels significantly associated with depression. (B) Functional connectivity of each lesion location to the rest of the brain was computed using resting state functional connectivity data from 1000 healthy controls. A focal region in the left dorsolateral prefrontal cortex showed greater functional connectivity to lesions of depressed subjects than to lesions of non-depressed subjects (depicted in red; voxel-level family-wise error [FWE] corrected $p < 0.05$). (C) Using normative connectome data, we examined the whole-brain functional connectivity of this region, generating a depression circuit. By definition, lesions from depressed subjects will intersect positive nodes of this network (sample lesion shown in violet) while lesions from non-depressed subjects will not (sample lesion shown in cyan). In panels B and C, the red-yellow coloration indicates regions positively connected to the region, while the blue-green coloration indicates regions negatively connected (anti-correlated) to the region. Network maps are thresholded at $T = \pm 5$ for ease of visualization (actual network maps were unthresholded). Z coordinates of slices in panel C: -25, -5, 15, 35, 55.

Figure 3. Lesion locations associated with depression intersect a brain circuit derived from independent lesion datasets. (A) The analysis shown in figure 2B was repeated five times, each time leaving out one of the five datasets. In all five analyses, a similar region in the left dorsolateral prefrontal cortex was significantly more connected to lesions of depressed subjects than to lesions of non-depressed subjects (depicted in red; voxel-level family-wise error [FWE] corrected $p < 0.05$). (B) and (C) The functional connectivity of each of these regions to the remainder of the brain was computed using a normative connective of 1000 healthy subjects, generating five depression circuits. The red-yellow and blue-cyan coloration depict positive connectivity and negative connectivity (anti-correlation) to the region, respectively, while green coloration depicts sample lesion locations from the excluded dataset. Depression circuits are thresholded at $T = \pm 5$ for ease of visualization (actual depression circuits for analysis are unthresholded). (D) Network damage scores, representing intersection of each lesion with the depression circuit generated from the other lesion datasets, was significantly higher for depressed subjects than control subjects.

Figure 4. Network damage score is associated with depression severity and prevalence. (A) All subjects were divided into three risk categories based on their network damage score. Mean depression score significantly differed across the risk categories and was highest in the high-risk group. (B) Prevalence of depression significantly differed across the risk categories and was highest in the high-risk group.

Figure 5. Our lesion-based depression circuit aligns with TMS sites used to treat post-stroke depression. Spheres indicate the stimulation locations used by prior transcranial magnetic stimulation studies that have successfully treated post-stroke depression. Our depression circuit is displayed on the cortical surface and thresholded at $T = \pm 5$ for ease of visualization (actual network is unthresholded).

Table 1. Subject Demographics.

Table 1

	Total Data	Naidech et al, 2016 (29)	Corbetta et al, 2015 (28)	Egorova et al, 2018 (30)	Gozzi et al, 2014 (17)	Koenigs et al, 2008 (7)
Total Subjects for Primary Analysis (Depressed/Non-Depressed)	358 (58/300)	33 (10/23)	87 (14/73)	49 (5/44)	45 (7/38)	144 (22/122)
Mean age (stdev)	59.3 (11.1)	58.6 (14.4)	53.8 (11.0)	68.1 (14.3)	63.5 (13.5)	58.5 (3.4)
Sex (% M, % F)	272 M (76%), 86 F (24%)	18 M (55%), 15 F (45%)	45 M (52%), 42 F (48%)	36 M (73%), 13 F (27%)	29 M (64%), 16 F (36%)	144 M (100%)
Lesion etiology		Intracerebral hemorrhage	Stroke (ischemic or hemorrhagic)	Ischemic stroke	Stroke (ischemic or intracerebral hemorrhagic)	Penetrating traumatic brain injury
Depression scale		Neuro-QOL depression scale (31)	Geriatric Depression Score Short Form (32)	Patient Health Questionnaire (PHQ-9) (33)	Hospital Anxiety and Depression Scale (34), followed by Mini-International Neuropsychiatric Interview (35)	Beck Depression Inventory II (36)
Depression threshold		Neuro-QOL T score ≥ 59.9 (equivalent to PHQ-9 ≥ 10)	GDSS ≥ 11	PHQ-9 ≥ 10	HADS ≥ 11, major depression per structured interview	BDI-II score ≥ 20
Threshold for Non-depressed status		Neuro-QOL T score ≤ 50.5 (equivalent to PHQ-9 ≤ 4)	GDSS ≤ 5	PHQ-9 ≤ 4	HADS < 11	BDI-II score ≤ 8
Time of Depression Assessment		Varied; 28 days, 3 months, or 12 months after hospital discharge	3 months after stroke	3 months after stroke	1 month after stroke	33-39 years following traumatic brain injury
Total Subjects for Continuous Analysis	461	51	100	63	51	196
Mean age (stdev)	59.3 (10.7)	61.1 (14.3)	53.6 (10.6)	67.5 (13.4)	62.6 (13.9)	58.3 (3.1)
Sex (% M, % F)	347 M (75 %) 114 F (25 %)	28 M (55%), 23 F (45%)	51 M (51%), 49 F (49%)	41 M (65%), 22 F (35%)	31 M (61%), 20 F (39%)	196 M (100%)

Figure 1

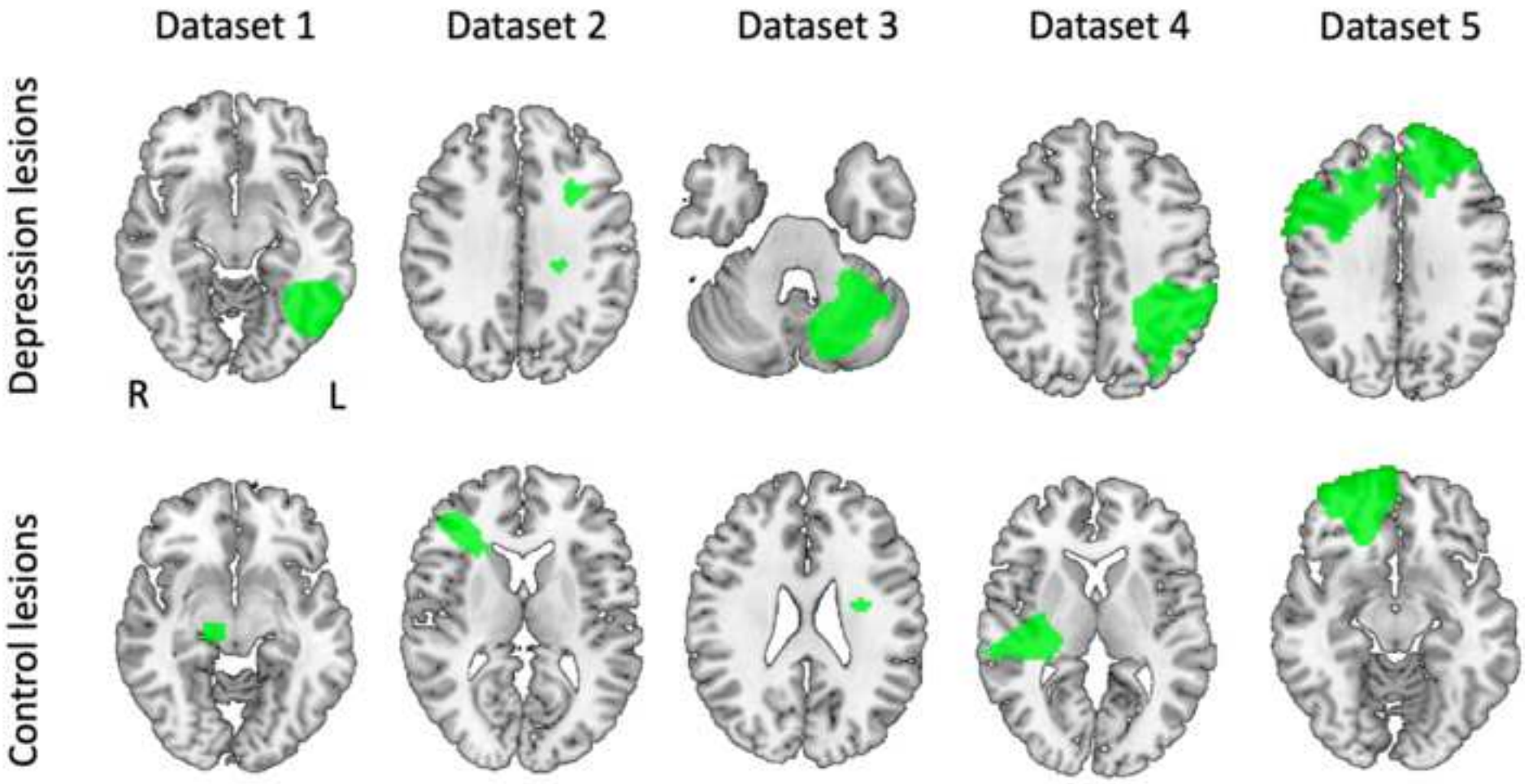
Dataset 1
Dataset 2
Dataset 3
Dataset 4
Dataset 5
Depression lesions
Control lesions
R
L

Figure 2

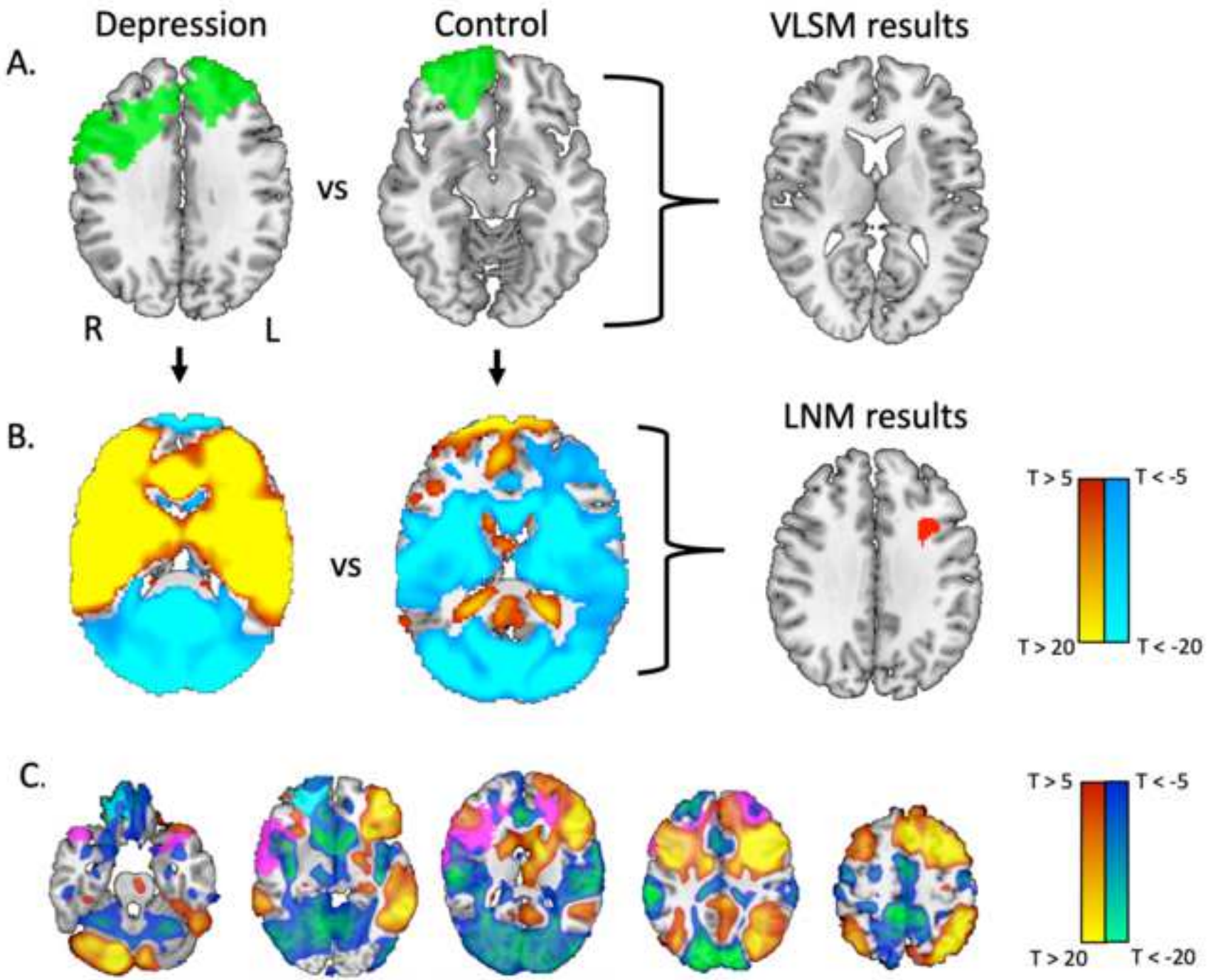
Depression
Control
VLSM results
A.
vs
R
L
B.
LNM results
vs
T > 5
T < -5
T > 20
T < -20
C.
T > 5
T < -5
T > 20
T < -20

Figure 3

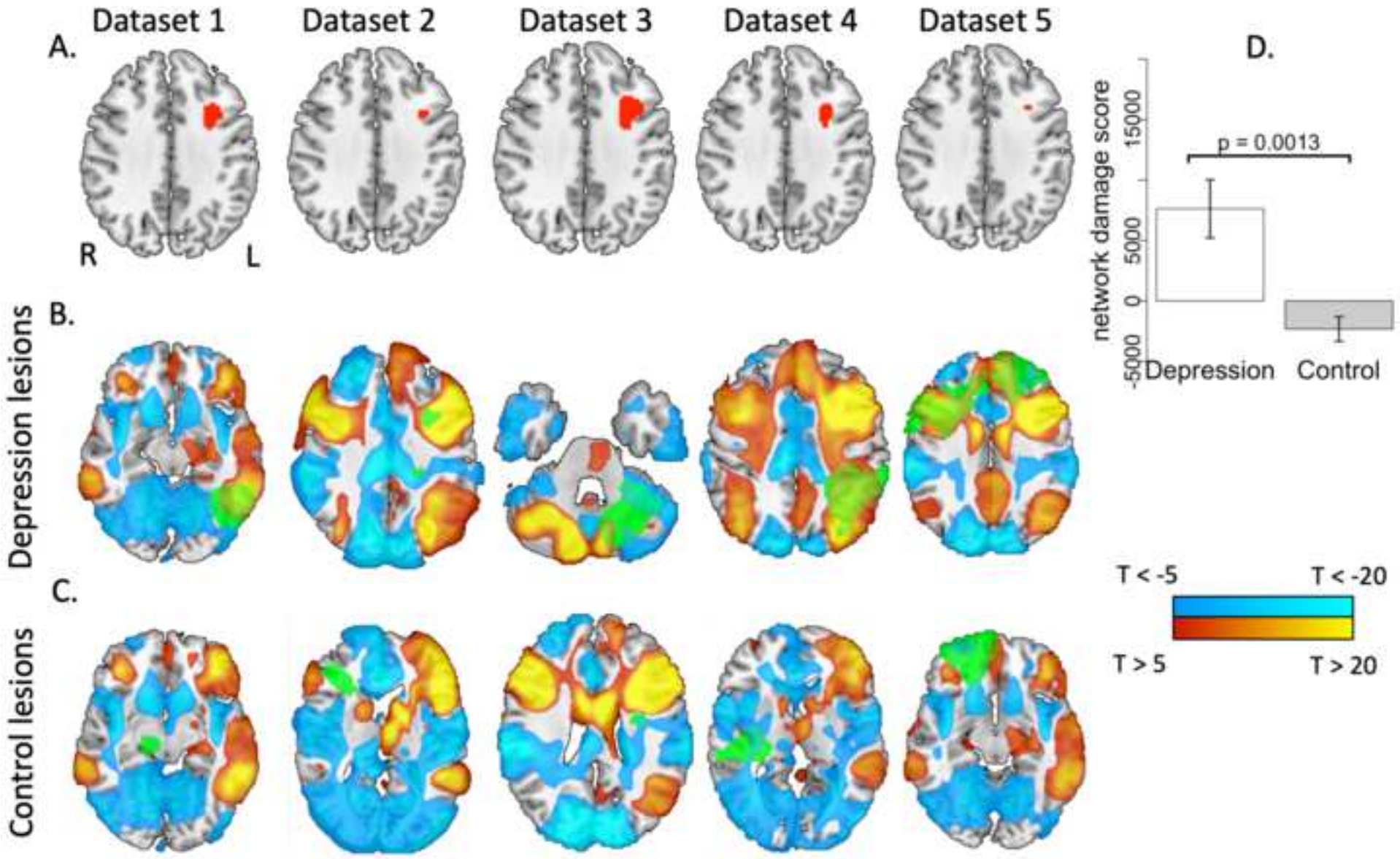
A.
Dataset 1
Dataset 2
Dataset 3
Dataset 4
Dataset 5
R
L
B.
Depression lesions
C.
Control lesions
D.
network damage score
15000
5000
0
-5000
p = 0.0013
Depression
Control
T < -5
T < -20
T > 5
T > 20

Figure 4

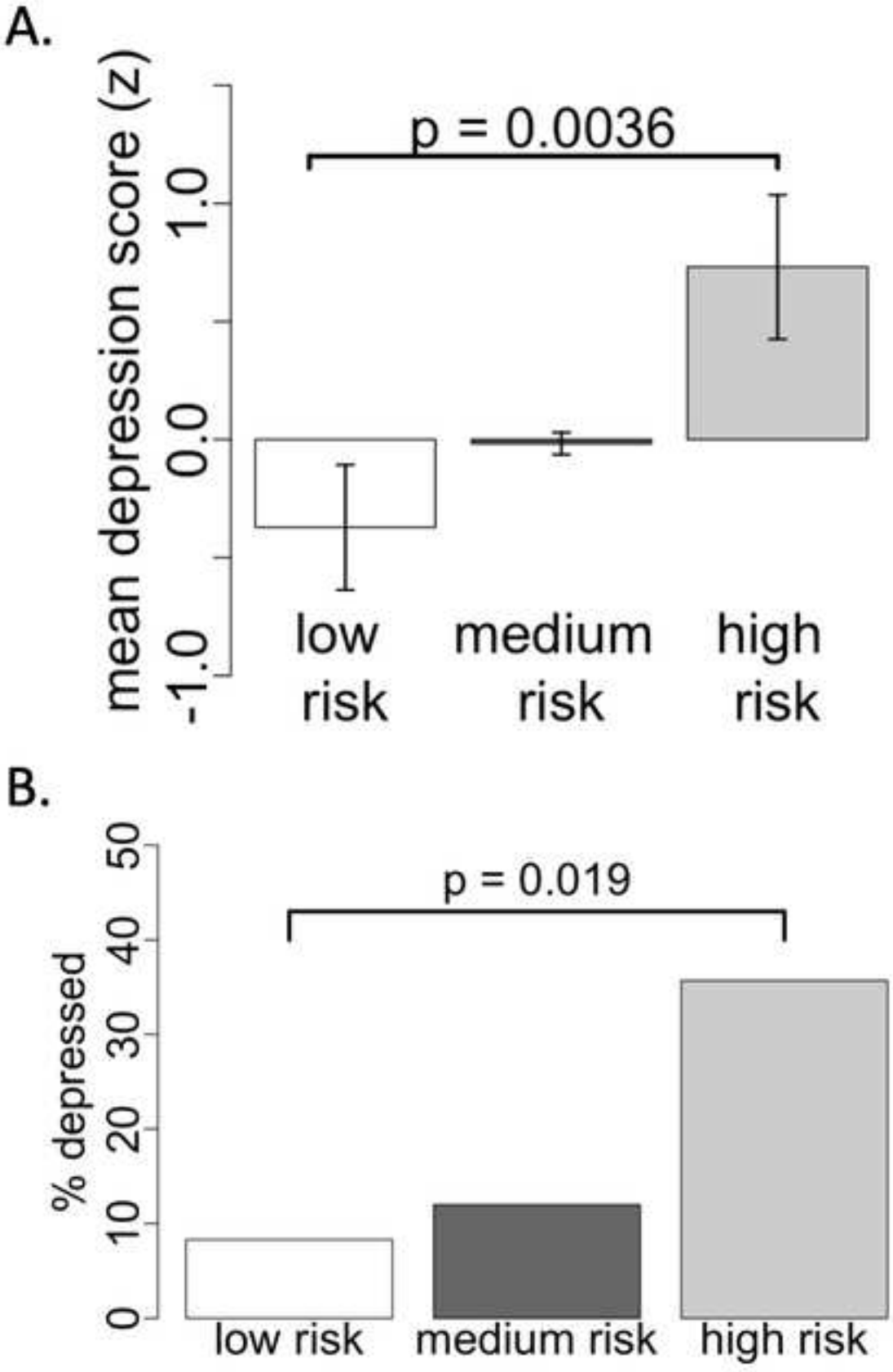
A.
mean depression score (z)
1.0
0.0
-1.0
p = 0.0036
low risk
medium risk
high risk
B.
% depressed
0
10
20
30
40
50
p = 0.019
low risk
medium risk
high risk

Figure 5

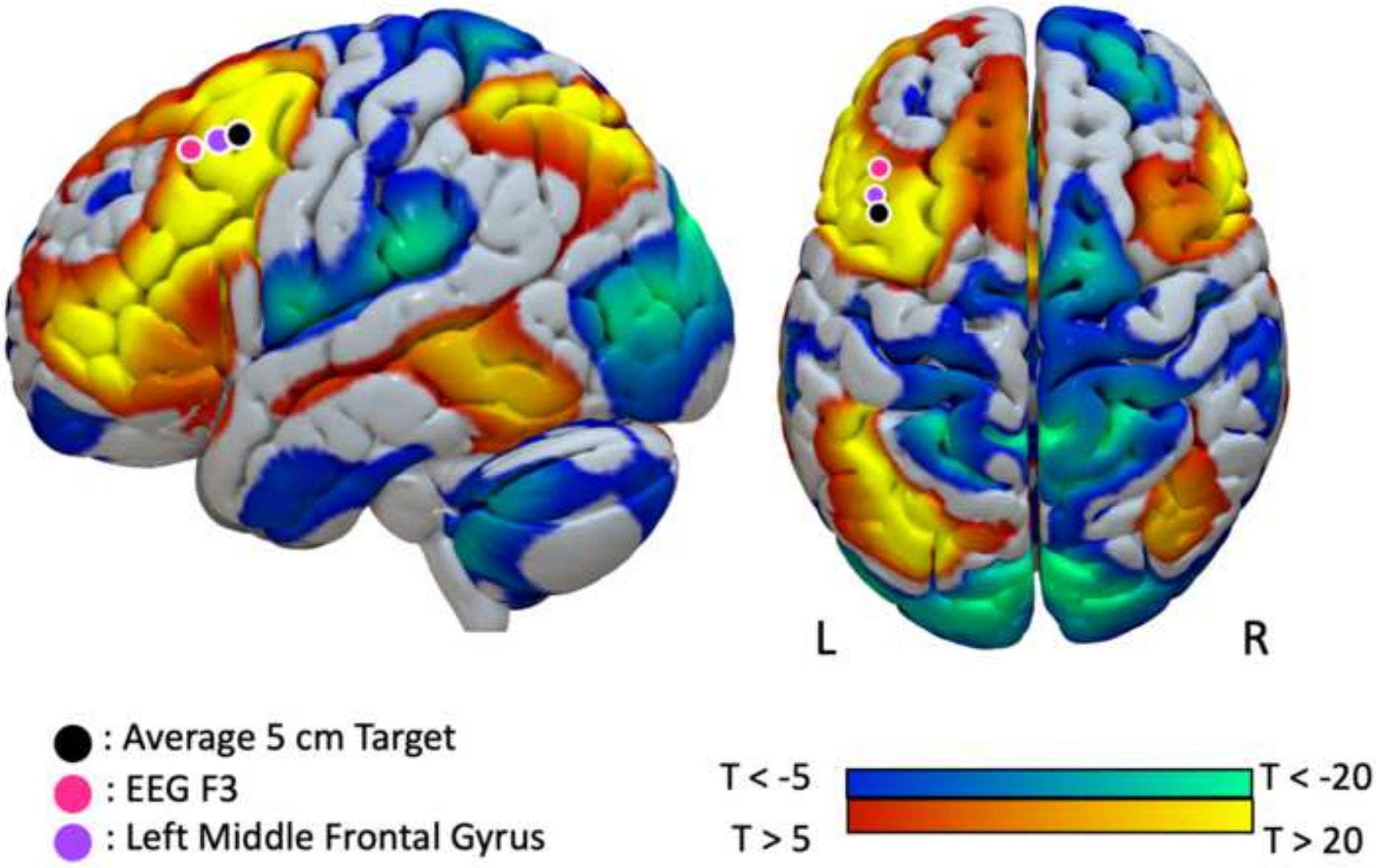
L
R
: Average 5 cm Target
: EEG F3
: Left Middle Frontal Gyrus
T < -5
T > 5
T < -20
T > 20

A Human Depression Circuit Derived From Focal Brain Lesions

Supplementary Information

Table of Contents

Supplementary Methods

Subjects and Lesions

The first dataset (1) consisted of subjects with intracerebral hemorrhage, assessed for depression using the computer adaptive test version of the Neuro Quality of Life scale and NIH Patient Reported Outcomes Measurement Information System (PROMIS) (2). Scores were collected at different time points (28 days, 3 months or 12 months after discharge) for different subjects. The scores are expressed as T scores centered on 50, with a standard deviation of +/- 10. We used an online tool that provides conversions between the Patient Health Questionnaire-9 (PHQ-9), a standard depression scale (3), and raw scores for the Neuro Quality of Life/PROMIS depression subscale. We found that standard thresholds of 4 and 10 for lack of depression and moderate depression on the PHQ-9 were equivalent to Neuro Quality of Life/PROMIS T scores of 50.5 and 59.9, respectively. Thus, we used these cut-offs to classify 10 subjects as depressed (mean = 65.0, standard deviation = 4.7) and 23 subjects as non-depressed (mean = 42.6, standard deviation =5.9) , excluding 18 subjects in the primary analysis. Information on pre-lesion history of depression or anti-depressant medication was not available in this dataset.

The second dataset (4) consisted of subjects with a first symptomatic stroke (ischemic or hemorrhagic) who had clinical evidence of neurological impairment, assessed for depression using the Geriatric Depression Score Short-Form (GDSS) (5) at 3 months and 1 year following stroke. Only the 3 month assessment was used for the current study. For our primary analysis, we classified subjects as "non-depressed" based on GDSS ≤ 5 or "moderate to severe depression" based on GDSS ≥ 11. These cutoffs were based on parameters set by the original authors of the GDSS (5), where GDSS ≥ 11 were classified as 'almost always depression' while those with scores > 5 and < 11 were classified as 'suggestive of depression'. This resulted in 14 subjects with moderate to severe depression (mean GDSS 12.0, standard deviation 1.0) and 73 without depression (mean GDSS 2.2, standard deviation 1.7), while excluding 13 with mild or questionable depression in the primary analysis. The dataset did contain information on pre-lesion history of depression but did not contain information on anti-depressant medication.

The third dataset (6) consisted of subjects with ischemic stroke, assessed three months after stroke with the Patient Health Questionnaire-9 (3). For our primary analysis, we classified subjects as "non-depressed" based on a PHQ-9 score of 4 or less, and "depressed" based on a PHQ-9 score of 10 or greater. These parameters were set by the authors of the PHQ-9 (3). This resulted in 5 subjects with moderate to severe depression (mean PHQ-9 = 13.0, standard deviation = 3.3) and 44 subjects without depression (mean PHQ-9 = 2.1, standard deviation = 1.4), while excluding 14 subjects with mild or questionable depression in the primary analysis. The study excluded subjects with any psychiatric history (including a history of depression) prior to stroke.

The fourth dataset (7) consisted of subjects with a first ischemic or intracerebral hemorrhagic stroke, evaluated for depression one month after stroke using the Hospital Anxiety and Depression Scale (HADS) (8). Those with a score of 11 or higher were evaluated with the Mini-International Neuropsychiatric Interview (MINI), a semi-structured

clinical interview (9), to determine presence of either major depression (major depressive-like episode following stroke) or minor depression (depressive features following stroke) per DSM-IV criteria. For our primary analysis, we classified subjects as "non-depressed" or "major depression" based on a previously published categorization of this dataset (7). This resulted in 7 subjects with major depression and 38 controls, excluding 6 individuals that were classified by the original authors as having 'minor depression' in the primary analysis. The dataset did contain information on pre-lesion history of depression. Three subjects included in our analysis were on antidepressant medication at the time of evaluation: one subject was a control, and the other two were classified as having 'minor depression' in the original dataset (equivalent to 'mild or questionable depression' in our analysis).

The fifth dataset (10) consisted of Vietnam War veterans with penetrating traumatic brain injury, assessed with the Beck Depression Inventory II about 33-39 years following their injury (11). For our primary analysis we classified subjects as "non-depressed" based on a BDI-II score ≤ 8 and "moderate to severe depression" based on a BDI-II score ≥ 20. These cutoffs were the same values used in prior analyses of this dataset (10). This resulted in 22 depressed subjects (mean BDI score 29.9, standard deviation 5.6), and 122 non-depressed subjects (mean BDI score 3.6, standard deviation 2.4), excluding 52 subjects with mild or questionable depression (BDI range 9-19) in the primary analysis. The dataset did not have information on pre-lesion history of depression or anti-depressant medication (10).

In total, the primary analysis dataset, which used a binary representation of depression status (depressed versus non-depressed), included 358 lesions. For analyses involving depression as a continuous measure, we included the 103 previously excluded subjects with mild or questionable depression (total N = 461). Depression scores within each dataset (NeuroQOL, GDSS, PHQ-9, HADS, BDI-II) were converted to z-scores (zero mean unit variance) to allow for cross-dataset analyses.

In analyses involving depression as a continuous measure, no subjects were excluded, retaining a total of 461 subjects.

Analysis of Lesion Location

To identify any lesioned voxel significantly associated with depression, we performed voxel lesion symptom mapping (VLSM) using NiiStat, a Matlab software package (https://github.com/neurolabusc/NiiStat) that can control for covariates (12).

NiiStat performs a pooled-variance t-test using general linear regression. For VLSM with NiiStat in our binary dataset, a total of 358 depression and control lesions were compared for voxels occurring in at least 5% of lesions, controlling for lesion size and dataset as nuisance regressors, with Freedman-Lane permutation for significance testing set at $p < 0.025$ one-tailed (equivalent to $p < 0.05$ two-tailed). The default setting of 2000 permutations was used. These parameters and statistical cutoffs were chosen based on published recommendations for VLSM analysis (13, 14). We performed this analysis using the Harvard-Oxford bilateral middle frontal gyrus (cutoff probability > 0%) as a mask.

We repeated the analysis using two DLPFC masks from prior lesion analyses ((10, 15); see below and Supplementary Figure 2), and using no mask at all (whole brain). The two DLPFC masks from prior lesion analyses consisted of the left anterior frontal region (Robinson *et al*, 1984) and the bilateral dorsolateral prefrontal region (Koenigs *et al*, 2008) (see Supplementary Figure 2, Supplementary Table 2). We then conducted this analysis with depression as a continuous measure and the entire dataset (461 subjects), again using the Harvard-Oxford bilateral middle frontal gyrus as a mask, then the two DLPFC masks from prior lesion analyses, and then no mask at all (see Supplementary Table 2).

We then replicated the prior lesion analyses of Robinson *et al* (15) and Koenigs *et al* (10) using their respective anatomical definitions and statistical methods in our binary dataset (N = 358). First, we used the definition of Robinson et al (15) to classify lesions according to where they fell with respect to certain percentages of the anterior-posterior (AP) distance: "The lesion was anterior if the anterior border of the lesion was rostral to 40 per cent of the AP distance and the posterior border was anterior to 60 per cent of the AP distance. On the other hand, a lesion was posterior if its anterior border was posterior to 40 per cent of the AP distance and the posterior border was caudal to 60 per cent of the AP distance." Lesions not fulfilling criteria for being either anterior or posterior were excluded. Chi-squared tests with Yates' continuity correction for statistical significance were performed to assess whether there was a difference in prevalence of depression between left anterior and left posterior lesions, between left anterior and right anterior lesions, or between right anterior and right posterior lesions.

Next, we replicated the analyses of Koenigs et al, 2008 (10) in our binary dataset (N=358). We classified lesions as bilateral dorsolateral prefrontal lesions, bilateral ventromedial prefrontal lesions, or non-prefrontal, while excluding unilateral vmPFC or dlPFC lesions: "The vmPFC ROI was defined as those areas of PFC inferior to $z = 0$ and medial to $x = 20$ and $x = -20$… The dlPFC ROI was defined as those areas of PFC superior to $z = 0$ and lateral to $x = -10$ and $x = 10$. A patient was included in the vmPFC group if his lesion occupied vmPFC in both hemispheres, but did not occupy any portion of dlPFC in either hemisphere. A patient was included in the dorsal PFC group if his lesion occupied dlPFC in both hemispheres, but did not occupy any portion of vmPFC in either hemisphere." We used Fisher's exact test to assess whether there was a significant difference in the proportion of depression among individuals with bilateral dlPFC lesions versus individuals with bilateral vmPFC lesions and versus non-prefrontal lesions.

Finally, we performed additional lesion laterality analyses. First, we created masks for each hemisphere by combining the Harvard Oxford cerebral cortex and cerebral white matter masks for each hemisphere, available in FSL 3.2.0. We then used these masks to classify lesions according to whether any voxels within them fell into the left cerebral hemisphere but not the right cerebral hemisphere, the right cerebral hemisphere but not the left, both, or neither. A chi-squared test with Yates' continuity correction for statistical significance was performed to assess whether there was a difference in prevalence of depression between left and right-sided lesions (excluding those lesions that fell into both or neither region).

Next, we used the Harvard Oxford middle frontal gyrus region of interest to create regions of interest representing the left and right middle frontal gyrus. We classified lesions according to whether any voxels within them fell into left middle frontal gyrus but not the right middle frontal gyrus, the right middle frontal gyrus but not the left middle frontal gyrus, both, or neither. A chi-squared test with Yates' continuity correction for statistical significance was performed to assess whether there was a difference in prevalence of depression between left middle frontal gyrus and right middle frontal gyrus lesions (excluding those lesions that fell into both or neither region).

Lesion Network Mapping

As described in the main text, we used each lesion image as a seed in a whole brain functional connectivity analysis in a normative dataset of 1000 subjects from the Brain Genomics Superstruct Project (https://dataverse.harvard.edu/dataverse/GSP) on whom resting state functional connectivity had been obtained using a 3T MRI. Processing of these scans has been fully described elsewhere (16), and included correction for motion and non-specific variance using global signal regression. To create a lesion network map, time series for voxels within the lesion were correlated with the time series from all other brain voxels in each of the 1000 healthy control subjects. Results were statistically combined across the 1000 subjects to create a voxelwise map of T values representing the strength and consistency of functional connectivity for each lesion location (Figure 2). Positive functional connectivity refers to a positive (direct) correlation of BOLD timeseries between regions or voxels, while negative functional connectivity refers to a negative (inverse) correlation of BOLD timeseries between regions or voxels.

Lesion network maps of 58 depressed versus 300 non-depressed subjects were statistically compared using a general linear model and permutation testing (Permutation Analysis of Linear Models in FSL 3.2.0), including lesion size and dataset as covariates (17, 18), and using the Harvard Oxford bilateral middle frontal gyrus (cutoff probability > 0%) as a mask. This region is provided in the Harvard-Oxford Cortical Atlas in FSLview version 3.2.0. We used a conservative voxel-level family-wise error correction for multiple comparisons, correcting for all brain voxels ($p < 0.05$). This is more stringent than the commonly used cluster-based correction which has been associated with false positives (19). We repeated this analysis with no mask and with two *a priori* DLPFC ROIs from the literature (Supplementary Figure 2) that we used in our analysis of lesion location, described in the previous section.

The significant results within the Harvard Oxford bilateral middle frontal gyrus mask were extracted as a seed, and the functional connectivity of this seed to the rest of the brain was computed using the normative connectome of 1000 healthy subjects. The resulting network map, which we term the "depression circuit", by definition encompasses lesion locations associated with depression while excluding lesion locations not associated with depression (peaks reported in Supplementary Table S3).

We then generated depression circuits from lesions only within each etiology (N = 52 for hemorrhagic stroke, N = 162 for ischemic stroke, and N=144 for penetrating traumatic brain injury). Following a similar process, we compared lesion network maps of depressed and non-depressed subjects within each etiology using a general linear model and permutation testing, including lesion size as a covariate, and using the Harvard-Oxford bilateral middle frontal gyrus as a mask. Due to loss of power in the smaller within-etiology sample sizes, results did not survive voxel-wise multiple comparison correction. Thus, different thresholds were used to define each DLPFC ROI. Seeds were generated by thresholding the uncorrected results at $p = 0.05$ (hemorrhagic lesions), $p = 0.001$ (ischemic lesions), and $p = 0.01$ (penetrating traumatic brain injury lesions). The functional connectivity of these seeds to the rest of the brain was computed using the normative connectome of 1000 subjects to generate depression circuits for each etiology. The spatial correlation of each depression circuit with the main depression circuit was assessed using a Pearson's correlation of the intensity at each voxel (Supplementary Figure S3).

An identical process was followed to generate a depression circuit from lesions of subjects with reported lack of history of depression prior to their lesion (N=168, of which N=24 depressed and N=144 non-depressed), using dataset and lesion size as covariates. Results of the comparison of lesion network maps of depressed and non-depressed individuals were thresholded at $p = 0.005$ uncorrected to generate a seed (Supplementary Figure S4A) that was then used to generate the depression circuit (Supplementary Figure S4B) using the normative connectome. The spatial correlation of this depression circuit with the primary depression circuit was assessed using a Pearson's correlation of the intensity at each voxel.

Leave-one-out Validation and Network Damage Scores

To ensure that our findings were not biased by any one of our five datasets, we performed a leave-one-dataset-out validation method. We statistically compared the lesion network maps of depressed and control subjects five times, each time leaving out one of the five datasets. For example, one of these five analyses used subjects in datasets 2-5 and excluded subjects in dataset 1, while another used subjects in datasets 1-4 and excluded subjects dataset 5. Each time, voxels that survived voxel-wise FWE correction were extracted as seeds for generating depression circuits (Figure 3A).

Then, we computed the functional connectivity of each of these seeds to the rest of the brain using the normative connectome data of 1000 subjects. Thus, we generated five network maps representing the circuitry of lesion-associated depression (Figure 3B and 3C), which we term 'depression circuits'. The spatial correlation between each pair of these maps was calculated as a Pearson's correlation between the intensities of all voxels in the maps.

We then assigned each subject a 'network damage score' using the depression circuit that was generated while excluding the dataset to which the subject belonged (Figure 3B and 3C). For example, network damage scores for subjects in Dataset 1 were assigned using the depression circuit that was created from Datasets 2-5. Each subject's

network damage score was calculated by summing the intensity values (T values) of those voxels in the depression circuit that overlapped with that subject's lesion. We regressed this score against lesion size and dataset and extracted the residuals to create an adjusted network damage score, which was used in all analyses.

Due to the non-normality of the network damage score, statistical significance for all analyses using this score was calculated using permutation testing. We examined whether the network damage score differed between depressed and control subjects using a permutation equivalent of a t-test (test of difference of means) (Figure 3D). We also assessed whether network damage score predicted depression using logistic regression. Analyses on the full cohort of subjects (N = 461) using a continuous measure of depression are described fully in the main text. Permutation testing was used for statistical significance due to non-normality of both the network damage score and the continuous depression measure.

Finally, we assessed whether lesion size alone predicted depression in these models. Lesion size was used as a predictor of binary depression status using a logistic regression model in the binary dataset (N=358), and as a predictor of continuous depression score using a Pearson's correlation in the continuous dataset (N=461).

Analyses dividing subjects into risk categories based on network damage score are described fully in the main text.

To set statistical significance using permutations, assignments of depressed or non-depressed status (or assignment of continuous depression measure) to subjects were randomly shuffled to create one million datasets. The test statistic of the correlation was calculated in all datasets to create a distribution of test statistics. The p value was the proportion of test statistics that were greater than the actual test statistic in our data.

Post-stroke Depression Treatment Targets

To identify studies of transcranial magnetic stimulation for post-stroke depression, we searched PubMed using the following search terms: "stroke", "depression" and "transcranial magnetic stimulation". This search yielded 113 English-language articles, whose abstracts we perused to identify 5 studies that successfully used transcranial magnetic stimulation with a primary endpoint of treating post-stroke depression in at least three subjects and provided adequate detail on the location of stimulation. We then identified the coordinates of the stimulation locations used in each of these studies. Two studies used 5 cm anterior to the motor hotspot ((20, 21), MNI coordinates: x = -41, y = 16, z = 54; coordinates obtained from (22)). Two studies (23, 24) used the left F3 electrode on the 10/20 EEG coordinate system (MNI coordinates: x = -37, y = 26, z = 49; coordinates obtained from (22)). The fifth study (25) used an approximation of the center of the middle frontal gyrus. To approximate the coordinates of that location, we identified the surface peak of the left Harvard Oxford middle frontal gyrus using the viewing software FSLeyes, within FSL 3.2.0 (MNI coordinates: x = -42, y = 20, z = 52). As a control, we used the vertex (Cz on EEG), frequently used as a control stimulation location in transcranial magnetic stimulation trials (coordinates: x = 1, y = -15, z = 74; (26)).

We created four 12-mm cone regions of interest (ROIs) centered on these stimulation locations by following previously published methodology (27). To summarize this methodology, concentric spheres were created with a radius of 2 mm, 4 mm, 7 mm, 9 mm, and 12 mm, centered on the coordinates of each stimulation location. The resulting structure was masked against the MNI 152 brain.

Using the normative connectome of 1000 subjects, we computed the resting state functional connectivity between the results of our lesion network mapping analysis (i.e., the region in the left DLPFC, 'LNM' in Figure 2B) and each cone ROI. This generated an r value representing the connectivity of each cone ROI with the results of our lesion network mapping analysis. We then compared the r value for each of the three successful stimulation targets with the r value for the vertex (a known 'unsuccessful' treatment target) using Hotelling's t-test and the cocor statistical package (28).

Supplementary Tables and Figures

Mask	N	Depression measure	# voxels analyzed	P value
Harvard-Oxford Middle Frontal Gyrus (bilateral)	358	binary	236	n.s.
Koenigs et al, 2008	358	binary	2291	n.s.
Robinson et al, 1984	358	binary	827	n.s.
No mask (whole brain)	358	binary	5917	n.s.
Harvard-Oxford Middle Frontal Gyrus (bilateral)	461	continuous	200	n.s.
Koenigs et al, 2008	461	continuous	3363	n.s.
Robinson et al, 1984	461	continuous	2113	n.s.
No mask (whole brain)	461	continuous	8386	n.s.

Supplementary Table S1. Voxel-based lesion-symptom mapping using NiiStat. Analyses regarding lesion location were performed in both the binary dataset (N=358), which excluded subjects with mild or questionable depression and used a binary variable to represent depressed or non-depressed status, and the continuous dataset, which included all subjects and used a continuous variable to represent depression severity.

	Left hemisphere	**Right hemisphere**	**Both**	**Neither**	**Total (%)**
Not depressed	91	101	88	20	300
Depressed	18	21	19	0	58
N (% of lesions)	109 (30%)	122 (34%)	107 (30%)	20 (6%)	358 (100%)
	Left MFG	**Right MFG**	**Both**	**Neither**	
Not depressed	31	53	8	208	300
Depressed	9	9	4	36	58
N (% of lesions)	40 (11%)	62 (17%)	12 (3%)	244 (68%)	358 (100%)

Supplementary Table S2. Lesion laterality in the binary (N=358) sample. Lesions were classified according to whether any voxels within them fell into the left cerebral hemisphere but not the right hemisphere, the right cerebral hemisphere but not the left, both, or neither (top four lines of table). They were also classified according to whether any voxels within them fell within the left middle frontal gyrus (MFG) but not the right, the right MFG but not the left, both, or neither (bottom four lines of table). There was no significant difference in prevalence of depression between lesions involving the left MFG and the right MFG, or between lesions involving the left and right cerebral hemispheres ($p > 0.05$).

Cluster	Location	Max T	Max X	Max Y	Max Z
1	Left middle frontal gyrus (left DLPFC)	207	-32	12	34
2	Right cerebellum	37	12	-74	-28
3	Right middle frontal gyrus (right DLPFC)	36	48	24	28
4	Lateral occipital cortex	36	-32	-70	48

Supplementary Table S3. Peaks of clusters within the depression circuit. Peaks were identified by thresholding the depression circuit at the lowest value that generated more than two clusters (T=36). Four clusters were generated, and the peaks of each are listed in this table.

Dataset	**1. Excluding Naidech et al, 2016**	**2. Excluding Corbetta et al, 2015**	**3. Excluding Egorova et al, 2018**	**4. Excluding Gozzi et al, 2004**	**5. Excluding Koenigs et al, 2008**
1. Excluding Naidech et al, 2016	1	0.84	0.97	0.98	0.96
2. Excluding Corbetta et al, 2015		1	0.92	0.85	0.78
3. Excluding Egorova et al, 2018			1	0.96	0.90
4. Excluding Gozzi et al, 2004				1	0.91
5. Excluding Koenigs et al, 2008					1

Supplementary Table S4. R values of Pearson's correlations between pairs of depression circuits. All five of our leave-one-dataset-out analyses yielded similar regions in the left DLPFC that survived voxel-level FWE correction. The connectivity of these regions to the rest of the brain was examined using a normative connectome of 1000 healthy subjects, generating five depression circuits representing lesion-associated depression. These five depression circuits were highly spatially correlated, as indicated by the high Pearson's correlations between any given pair of network maps.

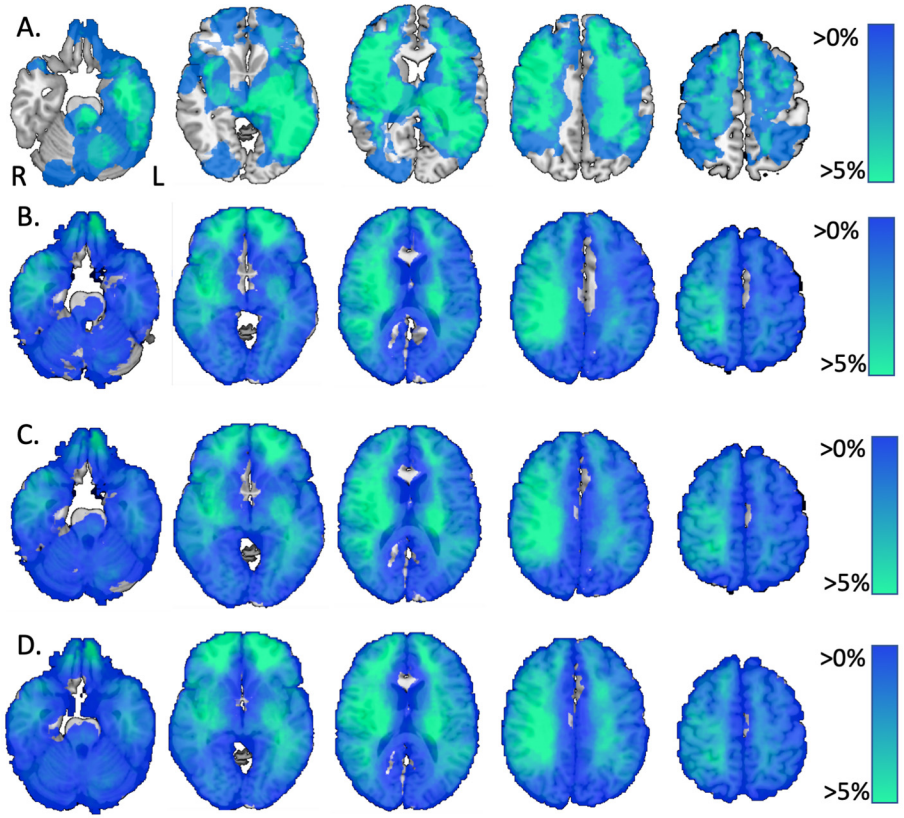

Supplementary Figure S1. **Lesion overlap maps, thresholded at 0 %.** Lesions were overlapped (summed) to depict the number of lesions overlapping at any given location.
A. Overlap map of lesions belonging to depressed subjects (N=58), max = 8.
B. Overlap map of lesions belonging to control subjects (N=300), max = 26.
C. Overlap map of depression and control lesions (excluding subjects with mild or questionable depression, N = 358), max = 32.
D. Overlap map of all lesions (N=461), max = 40.
Slice location: Z= -25, -5, 15, 35, 55

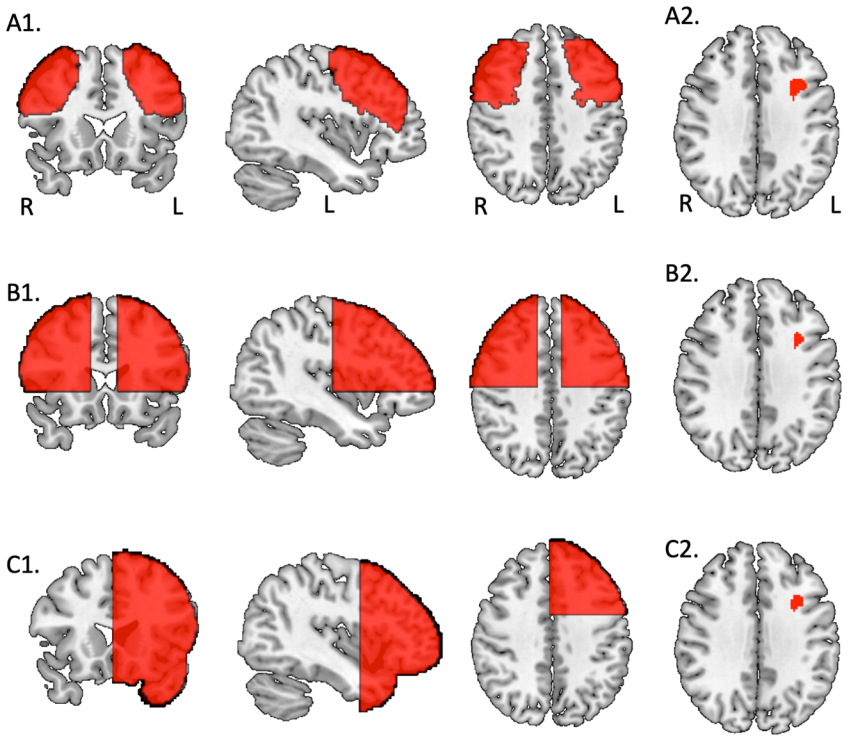

Supplementary Figure S2. A1. Harvard Oxford bilateral middle frontal gyrus (x=40, y=20, z=40).
A2. Results of general linear model comparing lesion network maps of depressed and control subjects, masking to Harvard Oxford Middle Frontal Gyrus (voxels with probability > 0%), with voxel-level FWE correction. Voxels in red survived multiple comparison correction (peak: T = 4.37, p_c = 0.0050, coordinates x = -32, y = 12, z = 36).
B1. Koenigs ROI (x=40, y=20, z=40) from Koenigs et al, 2008. B2. Results of general linear model comparing lesion network maps of depressed and control subjects, masking to Koenigs DLPFC, with voxel-level FWE correction. Voxels in red survived multiple comparison correction (peak: T = 4.37, p_c = 0.013, coordinates x = -32, y = 12, z = 36).
C1. Robinson ROI (x=40, y=20, z=40) from Robinson et al, 1984. C2. Results of general linear model comparing lesion network maps of depressed and control subjects, masking to Robinson ROI, with voxel-level FWE correction. Voxels in red survived multiple comparison correction (peak: T = 4.37, p_c = 0.0096; x = -32, y = 12, z = 36).

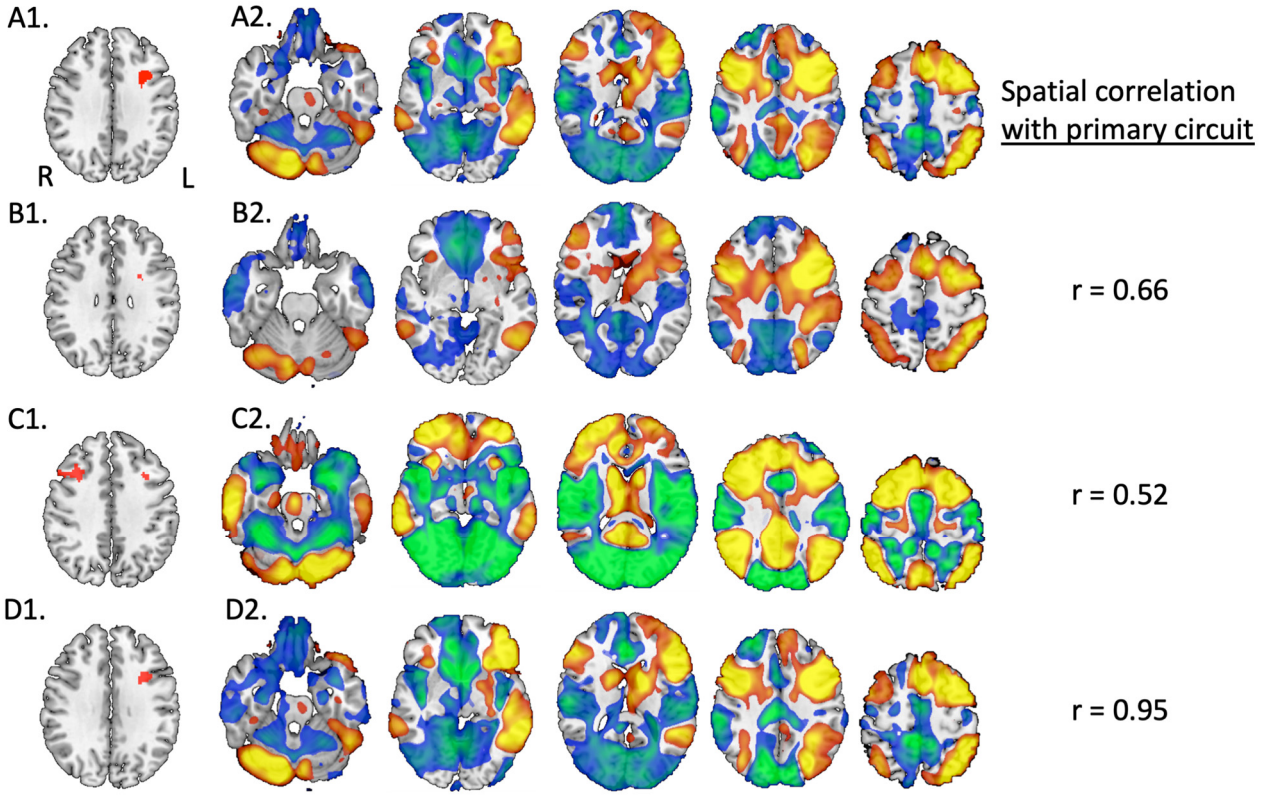

Supplementary Figure S3. Depression circuit compared to within-etiology depression circuits.
A1. 'Seed' used to generate depression circuit in primary analysis.
A2. Primary depression circuit generated using lesions of all etiologies (N = 358).
B1. Seed' used to generate depression circuit for hemorrhagic lesions.
B2. Depression circuit generated from hemorrhagic lesions (N = 52).
C1. Seed' used to generate depression circuit for ischemic lesions.
C2. Depression circuit generated from ischemic lesions (N = 162).
D1. Seed' used to generate depression circuit for penetrating traumatic brain injury lesions.
D2. Depression circuit generated from penetrating traumatic brain injury lesions (N=144).
z = -25, -5, 15, 35, 55 for slices of circuits. Thresholds for generating seeds are described in Supplementary Methods.

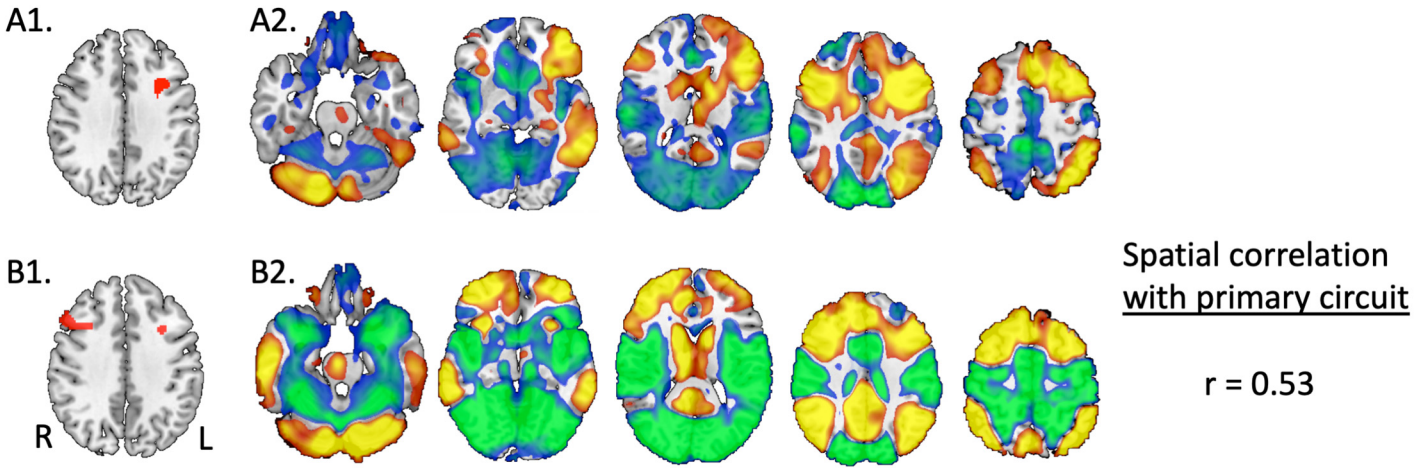

Supplementary Figure S4. Depression circuit compared to circuit of subjects (N=358) with confirmed lack of history of depression prior to lesion (N=168).
A1. Region of interest used as 'seed' to generate depression circuit in primary analysis.
A2. Axial slices of primary depression circuit at z = -25, -5, 15, 35, 55.
B1. Region of interest used as 'seed' to generate depression circuit for subset of subjects with confirmed lack of history of depression prior to lesion (N=168). Seed was generated by comparing lesion network maps of depressed and non-depressed subjects in PALM using a general linear model and thresholding the results at p (uncorrected) = 0.005.
B2. Axial slices of depression circuit generated from subjects with confirmed lack of history of depression prior to lesion (z = -25, -5, 15, 35, 55).

Supplementary References

1. Naidech AM, Polnaszek KL, Berman MD, Voss JL (2016): Hematoma Locations Predicting Delirium Symptoms After Intracerebral Hemorrhage. *Neurocrit Care*. 24:397-403.

2. Gershon RC, Lai JS, Bode R, Choi S, Moy C, Bleck T, et al. (2012): Neuro-QOL: quality of life item banks for adults with neurological disorders: item development and calibrations based upon clinical and general population testing. *Quality of life research : an international journal of quality of life aspects of treatment, care and rehabilitation*. 21:475-486.

3. Kroenke K, Spitzer RL, Williams JB (2001): The PHQ-9: validity of a brief depression severity measure. *J Gen Intern Med*. 16:606-613.

4. Corbetta M, Ramsey L, Callejas A, Baldassarre A, Hacker CD, Siegel JS, et al. (2015): Common behavioral clusters and subcortical anatomy in stroke. *Neuron*. 85:927-941.

5. Burke WJ, Roccaforte WH, Wengel SP (1991): The short form of the Geriatric Depression Scale: a comparison with the 30-item form. *J Geriatr Psychiatry Neurol*. 4:173-178.

6. Egorova N, Cumming T, Shirbin C, Veldsman M, Werden E, Brodtmann A (2018): Lower cognitive control network connectivity in stroke participants with depressive features. *Transl Psychiatry*. 7:4.

7. Gozzi SA, Wood AG, Chen J, Vaddadi K, Phan TG (2014): Imaging predictors of poststroke depression: methodological factors in voxel-based analysis. *BMJ Open*. 4:e004948.

8. Zigmond AS, Snaith RP (1983): The hospital anxiety and depression scale. *Acta Psychiatr Scand*. 67:361-370.

9. Sheehan DV, Lecrubier Y, Sheehan KH, Amorim P, Janavs J, Weiller E, et al. (1998): The Mini-International Neuropsychiatric Interview (M.I.N.I.): the development and validation of a structured diagnostic psychiatric interview for DSM-IV and ICD-10. *J Clin Psychiatry*. 59 Suppl 20:22-33;quiz 34-57.

10. Koenigs M, Huey ED, Calamia M, Raymont V, Tranel D, Grafman J (2008): Distinct regions of prefrontal cortex mediate resistance and vulnerability to depression. *J Neurosci*. 28:12341-12348.

11. Beck AT, Steer RA, Brown G (1996): Manual for the Beck Depression Inventory-II. San Antonion, TX: Psychological Corporation.

12. Stark BC, Yourganov G, Rorden C (2018): User Manual and Tutorial for NiiStat. http://wwwnitrcorg/projects/niistat.

13. Karnath HO, Sperber C, Rorden C (2018): Mapping human brain lesions and their functional consequences. *Neuroimage*. 165:180-189.

14. Sperber C, Karnath HO (2017): Impact of correction factors in human brain lesion-behavior inference. *Hum Brain Mapp*. 38:1692-1701.

15. Robinson RG, Kubos KL, Starr LB, Rao K, Price TR (1984): Mood disorders in stroke patients. Importance of location of lesion. *Brain*. 107 (Pt 1):81-93.

16. Yeo BT, Krienen FM, Sepulcre J, Sabuncu MR, Lashkari D, Hollinshead M, et al. (2011): The organization of the human cerebral cortex estimated by intrinsic functional connectivity. *J Neurophysiol*. 106:1125-1165.

17. Winkler AM, Ridgway GR, Webster MA, Smith SM, Nichols TE (2014): Permutation inference for the general linear model. *Neuroimage*. 92:381-397.

18. The MathWorks I (2015): MATLAB and Statistics Toolbox Release 2015b. Natick, Massachusetts.

19. Eklund A, Nichols TE, Knutsson H (2016): Cluster failure: Why fMRI inferences for spatial extent have inflated false-positive rates. *Proc Natl Acad Sci U S A*. 113:7900-7905.

20. VanDerwerker CJ, Ross RE, Stimpson KH, Embry AE, Aaron SE, Cence B, et al. (2018): Combining therapeutic approaches: rTMS and aerobic exercise in post-stroke depression: a case series. *Top Stroke Rehabil*. 25:61-67.

21. El Etribi A, El Nahas N, Nagy N, Nabil H (2010): Repetitive transcranial magnetic stimulation in post stroke depression. *Current Psychiatry*. 17:9-14.

22. Fox MD, Buckner RL, White MP, Greicius MD, Pascual-Leone A (2012): Efficacy of transcranial magnetic stimulation targets for depression is related to intrinsic functional connectivity with the subgenual cingulate. *Biol Psychiatry*. 72:595-603.

23. Gu SY, Chang MC (2017): The Effects of 10-Hz Repetitive Transcranial Magnetic Stimulation on Depression in Chronic Stroke Patients. *Brain stimulation*. 10:270-274.

24. Kim BR, Kim DY, Chun MH, Yi JH, Kwon JS (2010): Effect of repetitive transcranial magnetic stimulation on cognition and mood in stroke patients: a double-blind, sham-controlled trial. *Am J Phys Med Rehabil*. 89:362-368.

25. Jorge RE, Robinson RG, Tateno A, Narushima K, Acion L, Moser D, et al. (2004): Repetitive transcranial magnetic stimulation as treatment of poststroke depression: a preliminary study. *Biol Psychiatry*. 55:398-405.

26. Okamoto M, Dan H, Sakamoto K, Takeo K, Shimizu K, Kohno S, et al. (2004): Three-dimensional probabilistic anatomical cranio-cerebral correlation via the international 10-20 system oriented for transcranial functional brain mapping. *Neuroimage*. 21:99-111.

27. Fox MD, Liu H, Pascual-Leone A (2013): Identification of reproducible individualized targets for treatment of depression with TMS based on intrinsic connectivity. *Neuroimage*. 66:151-160.

28. Diedenhofen B, Musch J (2015): cocor: a comprehensive solution for the statistical comparison of correlations. *PLoS One*. 10:e0121945.